

An introduction to continuum mechanics and elastic wave propagation

lecture notes

Authors:

Mihály Dobróka, professor

Judit Somogyiné Molnár, research fellow

Editor: Judit Somogyiné Molnár, research fellow

Department of Geophysics

University of Miskolc

October 2014

Contents

1. Introduction	3
2. Continuum mechanical overview	3
2.1. Deformations and strains.....	4
2.2. The motion equation	11
2.3. Material equations.....	15
2.3.1. Material equation of the perfectly elastic body, stress dependent elastic parameters.....	15
2.3.2. Material and motion equation of Hooke-body	17
2.3.3. Fluid mechanical material models and their motion equations	20
2.3.4. Rheological material models and their motion equations.....	24
3. Wave propagation in elastic and rheological media	40
3.1. Low amplitude waves in ideal fluid	41
3.2. Low amplitude waves in isotropic linearly elastic medium	43
3.3. Low amplitude waves in viscous fluid.....	46
3.4. Low amplitude waves in Kelvin-Voigt medium	49
4. Elastic wave propagation.....	57
4.1. Describing the pressure dependence of longitudinal wave velocity	57
4.1.1. The pressure dependent acoustic velocity model	58
4.1.2. Experimental setting, technique and samples	60
4.1.3. Case studies	62
4.2. Describing the pressure dependence of quality factor.....	68
4.2.1. The pressure dependent seismic q model	70
4.2.2. The pressure dependent propagation velocity	74
4.2.3. Experimental samples.....	75
4.2.4. Estimation of model parameters appearing in the model.....	76
4.2.5. Inversion results	80

1. Introduction

Models are the simplified reality, where we keep the most important features and neglect the properties which do not or not substantially influence the examined process. In continuum physics the characteristics of the material are described by continuous functions which is inconsistent with the atomic structure. However in the description of many phenomena (e.g. elasticity, flows) the atomic and molecular descriptions are not necessary. The solution is that we introduce the phenomenological description method by averaging the atomic effects and take in so-called material characteristics "constants". These characteristics are usually non constants they are depend on temperature or other quantities. Thus we obtain a simplified - continuum - model of the material which is applied in many areas of rock mechanics and rock physics. The theory describing the mechanical properties of the continuum, the continuum mechanics is a phenomenological science.

2. Continuum mechanical overview

Based on the continuity hypothesis density functions assigned to extensive physical quantities (mass, momentum, energy) are considered mathematically as continuous functions of the location coordinates. Thus e.g. mass-density function ρ defined as follows

$$\rho(x_1, x_2, x_3) = \lim_{\Delta V \rightarrow 0} \frac{\Delta m}{\Delta V}, \quad (2.1)$$

where ΔV is a small volume around the point $P(x_1, x_2, x_3)$, Δm is the implied mass. The boundary transition $\Delta V \rightarrow 0$ is interpreted physically i.e. in the equation

$$dm = \rho dV$$

corresponding (2.1) the volume dV is „physically infinitesimal“. The boundary transition $\Delta V \rightarrow 0$ at low volume in mathematical sense leads to that the material belongs to ΔV will be qualitatively different. The boundary transition $\Delta V \rightarrow 0$ can be understood as ΔV tends to a volume V_0 which is quite large on the atomic scale but on the macroscopic scale it is small (small enough to be considered as point-like). It can be seen that the continuum mechanical and atomic description methods can be compatible. In continuum mechanics we get the simplified description of large groups of atoms thus we obtain relative simple equations. We deduce general laws hence further equations characterising the specific properties of the material are always necessary. These are the material equations containing so-called „material

constants" (e.g. elastic moduli) which reflect the neglected atomic features. In continuum mechanics the functions representing physical quantities are fractionally continuous, i.e. it may be exist surfaces in the media (eg. layer boundaries) along which the respective quantities suffer finite "hop". Boundary condition equations defined along these surfaces must be met.

2.1. Deformations and strains

After the axiom of the kinematics of deformable bodies the general movement (if it is quite small) of sufficiently small volume of the deformable body can be combined by a translation, a rotation and an extension or contraction took in three orthogonal directions. In the framework of continuum mechanics the displacement is given by the continuous vector $\bar{s}(r, t)$. To illustrate the meaning of the axiom of kinematics let us take up the coordinate system in the point P_0 of the deformable continuum and consider point P (originated from the small volume assumed around P_0) close to P_0 . During the movement of the continuum P pass through point P' satisfying the vector equation

$$\bar{r}' = \bar{r} + \bar{s},$$

where \bar{s} is the displacement vector „connencting” points P and P' . Assume that fracture surface is not extend between points P and P' . Then the two (adjacent) points can not move independently of one another, there is a „material relationship" between them defined by the continuum material.

This can be expressed mathematically that the displacement in point P is originated to characteristics refer to point P_0 , or in other words the displacement is exerted into series around point $P_0(0,0,0)$:

$$\begin{aligned} u_1 &= u_1^{(0)} + \left(\frac{\partial u_1}{\partial x_1}\right)_0 x_1 + \left(\frac{\partial u_1}{\partial x_2}\right)_0 x_2 + \left(\frac{\partial u_1}{\partial x_3}\right)_0 x_3 + \frac{1}{2} \left(\frac{\partial^2 u_1}{\partial x_1^2}\right)_0 x_1^2 + \dots \\ u_2 &= u_2^{(0)} + \left(\frac{\partial u_2}{\partial x_1}\right)_0 x_1 + \left(\frac{\partial u_2}{\partial x_2}\right)_0 x_2 + \left(\frac{\partial u_2}{\partial x_3}\right)_0 x_3 + \frac{1}{2} \left(\frac{\partial^2 u_2}{\partial x_1^2}\right)_0 x_1^2 + \dots \\ u_3 &= u_3^{(0)} + \left(\frac{\partial u_3}{\partial x_1}\right)_0 x_1 + \left(\frac{\partial u_3}{\partial x_2}\right)_0 x_2 + \left(\frac{\partial u_3}{\partial x_3}\right)_0 x_3 + \frac{1}{2} \left(\frac{\partial^2 u_3}{\partial x_1^2}\right)_0 x_1^2 + \dots, \end{aligned} \quad (2.1.1)$$

where ... means other "higher parts" appearing in the expansion and index 0 indicating next to the derivatives refers to that the derivatives should take in the origin (P_0).

In the axiom of kinematics we talk about the "displacement of sufficiently small volume". It means that in equations (2.1.1) the "higher parts" containing the powers and products of coordinates x_1, x_2, x_3 are negligible, i.e. we live with a linear approximation. In addition, we also assume that the first derivatives are small in the sense that their product and powers are negligible. Herewith (2.1.1) takes the following form

$$u_i = u_i^{(0)} + \sum_{j=1}^3 \left(\frac{\partial u_i}{\partial x_j} \right)_0 x_j, \quad i = 1, 2, 3 \quad (2.1.2)$$

In the followings, we will apply the so-called Einstein's convention with which (2.1.2) can be written as

$$u_i = u_i^{(0)} + \left(\frac{\partial u_i}{\partial x_j} \right)_0 x_j$$

i.e. if an index (or indices) in an expression occurs twice we should sum from 1 to 3. In the followings the index 0 beside the derivatives $\left(\frac{\partial u_i}{\partial x_j} \right)_0$ is omitted, so

$$u_i = u_i^{(0)} + \frac{\partial u_i}{\partial x_j} x_j. \quad (2.1.3)$$

The derivative tensor $\frac{\partial u_i}{\partial x_j}$ can be divided into symmetric and antisymmetric parts as

$$\frac{\partial u_i}{\partial x_j} = \frac{1}{2} \left(\frac{\partial u_i}{\partial x_j} - \frac{\partial u_j}{\partial x_i} \right) + \frac{1}{2} \left(\frac{\partial u_i}{\partial x_j} + \frac{\partial u_j}{\partial x_i} \right).$$

With this we obtain the following equation for the (2.1.3) displacements

$$u_i = u_i^{(0)} + \frac{1}{2} \left(\frac{\partial u_i}{\partial x_j} - \frac{\partial u_j}{\partial x_i} \right) x_j + \frac{1}{2} \left(\frac{\partial u_i}{\partial x_j} + \frac{\partial u_j}{\partial x_i} \right) x_j, \quad (2.1.4)$$

where $u_i^{(0)}$ is the same for any points of the small volume taken around P_0 , i.e. $u_i^{(0)}$ means homogeneous translation for the movement of these points

$$\bar{s}_{\text{transz}} = (u_1^{(0)}, u_2^{(0)}, u_3^{(0)}).$$

Introducing the notation

$$\delta\bar{\varphi} = \frac{1}{2} \text{rot } \bar{s} \quad (2.1.5)$$

it can be easily seen that the second part in (2.1.4) equals to the vectorial product $[\delta\bar{\varphi}, \bar{r}]$ which describes the rotational displacement

$$\bar{s}_{\text{rot}} = \left[\frac{1}{2} \text{rot } \bar{s}, \bar{r} \right].$$

Thus, it is obvious that the third part of (2.1.4) provides the deformation displacements

$$\bar{s}_{\text{def}} = \{u_1^{(d)}, u_2^{(d)}, u_3^{(d)}\},$$

where

$$u_i^{(d)} = \frac{1}{2} \left(\frac{\partial u_i}{\partial x_j} + \frac{\partial u_j}{\partial x_i} \right) x_j. \quad (2.1.6)$$

Introducing the notation

$$\varepsilon_{ij} = \frac{1}{2} \left(\frac{\partial u_i}{\partial x_j} + \frac{\partial u_j}{\partial x_i} \right) \quad (2.1.7)$$

(2.1.6) can be reformulated as

$$u_i^{(d)} = \varepsilon_{ij} x_j, \quad (2.1.8)$$

where the symmetrical second-order tensor ε_{ij} called deformation tensor.

To clarify the components of the deformation tensor take a material line in unit length along the coordinate axis x_i of the original coordinate system and denote it as vector

$\bar{r} = \bar{i} = (1, 0, 0)$. During deformation this transforms to vector

$$\bar{r}'_i = (1 + \varepsilon_{11}, \varepsilon_{12}, \varepsilon_{13}) \quad (2.1.9)$$

due to equation (2.1.8), according to the equation

$$\bar{r}' = \bar{r} + \bar{s}.$$

Hence the relative expansion is

$$\frac{|\bar{r}'| - |\bar{i}|}{|\bar{i}|} = \sqrt{(1 + \varepsilon_{11})^2 + \varepsilon_{12}^2 + \varepsilon_{13}^2} - 1 \approx \varepsilon_{11},$$

as we limit ourselves to small deformations ($\varepsilon_{11}, \varepsilon_{22}, \varepsilon_{33} \ll 1$).

Thus deformation ε_{11} means the expansion of the section in unit length taken along axis x_1 or in other words the relative expansion measured along axis x_1 . Elements $\varepsilon_{22}, \varepsilon_{33}$ have similar meaning. Elements in the main diagonal of the deformation tensor give the relative expansion of the material line sections falling into axes x_1, x_2, x_3 . To investigate the meanings of the elements outside the main diagonal let us take the unit vector \vec{j} falling into the direction of the coordinate axis x_2 which after deformation transforms into vector

$$\vec{r}'_2 = (\varepsilon_{21}, 1 + \varepsilon_{22}, \varepsilon_{32}).$$

By equation (2.1.9) plus forming the scalar product (\vec{r}'_1, \vec{r}'_2) and neglecting the squares as well as products of deformations one obtains

$$(\vec{r}'_1, \vec{r}'_2) \approx 2\varepsilon_{12}.$$

Applying

$$(\vec{r}'_1, \vec{r}'_2) \approx |\vec{r}'_1| |\vec{r}'_2| \cos \alpha,$$

where $|\vec{r}'_1| \approx |\vec{r}'_2| \approx 1$ and the angle between the two vectors is

$$\delta = \frac{\pi}{2} - \alpha$$

results as

$$\delta = 2\varepsilon_{12},$$

where $\sin \delta \approx \delta$ was used to small angles. Ergo deformation ε_{12} is the half of the angle change which is suffered by the line section taken in the originally perpendicular directions \vec{i} and \vec{j} .

Take a prism with a volume $V = abc$ and with edges parallel to the coordinate axes in the undeformed continuum! The volume of the prism generated during deformation will be approximately

$$V = (1 + \varepsilon_{11})(1 + \varepsilon_{22})(1 + \varepsilon_{33})abc$$

i.e. the relative volume change is

$$\Theta = \frac{V' - V}{V} = \varepsilon_{11} + \varepsilon_{22} + \varepsilon_{33}.$$

The sum of the elements in the main diagonal of the deformation tensor (a.k.a. the spur of the deformation tensor or the invariant of the first scalar) means the relative volume change. Contrariwise one can express it with equation

$$\Theta = \varepsilon_{qq}$$

(summarize to q !), or on the basis of definition (2.1.7) of the deformation tensor

$$\Theta = \frac{\partial u_1}{\partial x_1} + \frac{\partial u_2}{\partial x_2} + \frac{\partial u_3}{\partial x_3} = \operatorname{div} \bar{s}. \quad (2.1.10)$$

This quantity is unchanged during coordinate transformation.

To characterize the deformations it is used to introduce the spherical tensor

$$E_{ik}^{(0)} = \frac{1}{3} \varepsilon_{qq} \delta_{ik} \quad (2.1.11)$$

and the deformation deviatoric tensor

$$E_{ik} = \varepsilon_{ik} - \frac{1}{3} \varepsilon_{qq} \delta_{ik}, \quad (2.1.12)$$

where δ_{ik} is a unit tensor i.e.

$$\delta_{ik} = \begin{cases} 1, & \text{if } i = k \\ 0, & \text{if } i \neq k \end{cases}.$$

The name is originated in that the second-order tensor surface ordered to the deformation spherical tensor is sphere. With this tensor the pure volume change can be separated from the deformations. The remaining part of deformations E_{ik} shows the deviation from the pure volume change, i.e. the so-called distortion. It is obvious according to (2.1.12) that $E_{qq} = 0$.

The decomposition of the deformation tensor

$$\varepsilon_{ik} = E_{ik} + E_{ik}^{(0)} \quad (2.1.13)$$

means also the pick apart it to the volume change-free "pure distortion" and the pure volume change. The dynamic interpretation of the movement of the continuum requires to introduce the force densities. Experiences show that the forces affecting on the continuum can be divided into two types: volume and surface forces. The volume force $d\bar{F}$ - affecting to the

continuum contains the (physically) infinitesimal volume element dV took at a given point of the space - can be written as

$$d\vec{F} = \vec{f}^* dV ,$$

where \vec{f}^* is the volumetric force density. The integral of the volumetric force density

$$\vec{F} = \int_V \vec{f}^* dV$$

gives the force affected to finite volume. The volumetric force density can be calculated otherwise by the definition

$$\vec{f}^* = \lim_{\Delta V \rightarrow 0} \frac{\Delta \vec{F}}{\Delta V} .$$

There are forces that are physically directly proportional not to the volume, but the mass. These can be characterized by the mass force density

$$\vec{f} = \lim_{\Delta m \rightarrow 0} \frac{\Delta \vec{F}}{\Delta m} ,$$

where Δm is the mass contained in the volume ΔV . With which

$$\vec{f} = \lim_{\Delta V \rightarrow 0} \frac{\Delta V}{\Delta m} \frac{\vec{F}}{\Delta V} = \frac{1}{\rho} \vec{f}^*$$

or otherwise

$$\vec{f}^* = \rho \vec{f} . \tag{2.1.14}$$

Another class of forces arising in the continuum are the surface forces. The surface force density can be formulated as

$$\vec{\sigma}_n = \lim_{\Delta A \rightarrow 0} \frac{\Delta \vec{F}}{\Delta A} , \tag{2.1.15}$$

where the boundary transition $\Delta A \rightarrow 0$ can be interpreted as ΔA tends to a so small surface A_0 which is negligible (point-like) in macroscopic point of view but it is very large compared to the atomic cross section. Otherwise equation (2.1.15) can be written as

$$\Delta \vec{F} = \vec{\sigma}_n dA . \tag{2.1.16}$$

In (2.1.16) „index” \vec{n} implies that the surface force at a given space depends on not only the extent of the surface but its direction - characterized by the normal unit vector \vec{n} - too. Based on (2.1.16) the force affected on the finite surface A can be calculated as

$$\vec{F} = \int_A \vec{\sigma}_{\vec{n}} dA. \quad (2.1.17)$$

Since the unit normal vector \vec{n} can point to infinite number of directions apparently the knowledge of infinitely many surface force densities is necessary to provide the surface forces. However it can be proved that

$$\vec{\sigma}_{\vec{n}} = \vec{\sigma}_{x_1} n_1 + \vec{\sigma}_{x_2} n_2 + \vec{\sigma}_{x_3} n_3. \quad (2.1.18)$$

This equation shows that if we know in one point the surface force density $\vec{\sigma}_{x_i}$ affected on three orthogonal coordinate plane then surface force densities (also known as strains) affected on any \vec{n} directional surface can be calculated by the help of equation (2.1.18).

Introducing the notations

$$\vec{\sigma}_{\vec{n}} = (\sigma_{n_1}, \sigma_{n_2}, \sigma_{n_3})$$

$$\vec{\sigma}_{x_1} = (\sigma_{11}, \sigma_{12}, \sigma_{13})$$

$$\vec{\sigma}_{x_2} = (\sigma_{21}, \sigma_{22}, \sigma_{23})$$

$$\vec{\sigma}_{x_3} = (\sigma_{31}, \sigma_{32}, \sigma_{33})$$

(2.1.18) can be written as

$$\sigma_{n_i} = \sigma_{ij} n_j, \quad (i = 1, 2, 3) \quad (2.1.19)$$

(where according to our agreement one has to summarize to j from 1 to 3). Ergo after (2.1.19) to characterize the surface force density the second-order tensor σ_{ij} is introduced which is the j -th component of the strain vector affected on the surface supplied with a normal pointing to the direction of the i -th coordinate axis. It can be proved that this tensor is symmetric, i.e.

$$\sigma_{ij} = \sigma_{ji}.$$

The elements $\sigma_{11}, \sigma_{22}, \sigma_{33}$ in the main diagonal of the tensor are normal directional (tensile or compressive) stresses, the outside elements $\sigma_{12}, \sigma_{13}, \sigma_{23}$ are tangential (shear or slip)

stresses. Similarly at the deformation tensor one can produce the stress tensor as the sum of the deviator and the stress spherical tensors.

$$\sigma_{ik} = T_{ik} + T_{ik}^{(0)}, \quad (2.1.20)$$

where

$$T_{ik}^{(0)} = \frac{1}{3} \sigma_{qq} \delta_{ik}, \quad T_{ik} = \sigma_{ik} - \frac{1}{3} \sigma_{qq} \delta_{ik}, \quad (2.1.21)$$

and σ_{qq} is the sum of the elements in the main diagonal of the stress tensor.

2.2. The motion equation

At the deduction of the motion equation of deformable continua the starting point is Newton's II. law which says that the time-derivate of the impulse of the body equals to the sum of the arose forces

$$\frac{d\vec{I}}{dt} = \sum \vec{F}.$$

The impulse of the body can be determined by the formula

$$\vec{I} = \int_V \vec{i} dV$$

where

$$\vec{i} = \lim_{\Delta V \rightarrow 0} \frac{\vec{v} \Delta m}{\Delta V} = \rho \vec{v}$$

is the volumetric impulse density, while $\vec{v} = \frac{\partial \vec{s}}{\partial t}$ is the velocity. The resultant force affecting the body is the sum of the volume and surface forces, i.e.

$$\sum \vec{F} = \int_V \rho \vec{f} dV + \oint_A \vec{\sigma}_{\vec{n}} dA.$$

The integral form of the motion equation can be written as

$$\frac{d}{dt} \int_{V(t)} \rho \vec{v} dV = \int_{V(t)} \rho \vec{f} dV + \oint_{A(t)} \vec{\sigma}_{\vec{n}} dA,$$

where $V(t)$, $A(t)$ are the volume as well as surface moving together with the continuum. To the i -th coordinate of the vector equation one can obtain

$$\frac{d}{dt} \int_{V(t)} \rho v_i dV = \int_{V(t)} \rho f_i dV + \oint_{A(t)} \sigma_{n_i} dA . \quad (2.2.1)$$

To transform the latter equation use the identity

$$\frac{d}{dt} \int_{V(t)} \phi dV = \int_{V(t)} \left\{ \frac{\partial \phi}{\partial t} + \text{div}(\phi \vec{v}) \right\} dV$$

and the Gauss-Osztogradskij thesis

$$\oint_{A(t)} \sigma_{n_i} dA = \oint_{A(t)} \sigma_{ij} n_j dA = \oint_{A(t)} \sigma_{ij} dA_j = \oint_{A(t)} \bar{\sigma}_i d\bar{A} = \int_{V(t)} \text{div} \bar{\sigma}_i dV ,$$

where $dA_j = n_j dA$ and

$$\bar{\sigma}_i = (\sigma_{i1}, \sigma_{i2}, \sigma_{i3})$$

denotes - as a formal vector - the i-th row of the stress tensor. Here the equation (2.1.19) was also used. Now the motion equation (2.2.1) can be written as

$$\int_{V(t)} \left\{ \frac{\partial(\rho v_i)}{\partial t} + \text{div}(\bar{v} \rho v_i) - \rho f_i - \text{div} \bar{\sigma}_i \right\} dV = 0.$$

Hence volume $V(t)$ is arbitrary, from the disappearance of the integral one can infer to the disappearance of the integrand

$$\frac{\partial(\rho v_i)}{\partial t} + \text{div}(\rho v_i \bar{v}) = \rho f_i + \text{div} \bar{\sigma}_i ,$$

otherwise

$$\frac{\partial(\rho v_i)}{\partial t} + \text{div}(\rho v_i \bar{v}) = \rho f_i + \frac{\partial \sigma_{ik}}{\partial x_k}. \quad (2.2.2)$$

This is the local form of the motion equation of the deformable continuum, also known as the balance equation of the impulse.

In continuum theory equations describing the transport of extensive quantities can be commonly reformulated to the format of the continuity equation. If the bulk density of a quantity is w then the convective current density of the given quantity is denoted as $\vec{J}_w^{(konv)} = w \vec{v}$. $\vec{J}_w^{(kond)}$ represents the conductive (connected to macroscopic motions) current density. Then the balance equation of quantity w is

$$\frac{\partial w}{\partial t} + \operatorname{div}(\bar{J}_w^{konv} + \bar{J}_w^{kond}) = 0,$$

or if it has sources (or sinks)

$$\frac{\partial w}{\partial t} + \operatorname{div}(\bar{J}_w^{konv} + \bar{J}_w^{kond}) = \alpha, \quad (2.2.3)$$

where α is the source strength which provides the quantity of w produced or absorbed in unit volume per unit time.

Introducing the convective $\bar{J}_{imp}^{(konv)} = \rho v_i \bar{v}$ and conductive $\bar{J}_{imp}^{(kond)} = -\{\sigma_{ik}\}$ impulse-current density vectors equation (2.2.2) can be written as

$$\frac{\partial(\rho v_i)}{\partial t} + \operatorname{div}(\bar{J}_{imp}^{(konv)} + \bar{J}_{imp}^{(kond)}) = \rho f_i.$$

Ergo the stress tensor (that of onefold) is physically the conductive impulse current density, while volumetric force density ρf_i plays the role of the source strength of the impulse. It is well-known that similar balance equation can be formed to (mass) density $\rho_{(j)}$ of the j-th component of a fluid compound

$$\frac{\partial \rho_{(j)}}{\partial t} + \operatorname{div}(\bar{J}_m^{(konv)} + \bar{J}_m^{(kond)}) = \gamma_{(j)},$$

where the convective mass flow density is $\bar{J}_m^{(konv)} = \rho_{(j)} \bar{v}$. The conductive mass flow density provides a way to describe the diffusive motions, source strength $\gamma_{(j)}$ refers to the chemical reaction which gives the production of the j-th component. To one-component fluid by neglecting the source strength the continuity equation

$$\frac{\partial \rho}{\partial t} + \operatorname{div}(\rho \bar{v}) = 0 \quad (2.2.4)$$

provides the balance equation of the mass. By transforming the left side of equation (2.2.2) one can obtain

$$v_i \left\{ \frac{\partial \rho}{\partial t} + \operatorname{div}(\rho \bar{v}) \right\} + \rho \left\{ \frac{\partial v_i}{\partial t} + \bar{v} \operatorname{grad} v_i \right\} = \rho f_i + \frac{\partial \sigma_{ik}}{\partial x_k},$$

where the identity

$$\operatorname{div}(a \bar{A}) = a \operatorname{div} \bar{A} + \bar{A} \operatorname{grad} (a)$$

was used (where a and \bar{A} are the continuous function of the three spatial coordinates). By taking into consideration the continuity equation, (2.2.2) can be written as

$$\rho \left\{ \frac{\partial v_i}{\partial t} + \bar{v} \text{grad } v_i \right\} = \rho f_i + \frac{\partial \sigma_{ik}}{\partial x_k}.$$

We call the partial derivate $\frac{\partial}{\partial t}$ otherwise local, while the operator $\bar{v} \text{grad}$ is the convective derivate and

$$\frac{d}{dt} = \frac{\partial}{\partial t} + \bar{v} \text{grad}$$

is the substantial derivate. Hereby the motion equation can be written as

$$\rho \frac{dv_i}{dt} = \rho f_i + \frac{\partial \sigma_{ik}}{\partial x_k}. \quad (2.2.5)$$

In solid continua the convection can be negligible thus $\frac{d}{dt} \approx \frac{\partial}{\partial t}$ and the motion equation is

$$\rho \frac{\partial^2 u_i}{\partial t^2} = \rho f_i + \frac{\partial \sigma_{ik}}{\partial x_k}. \quad (2.2.6)$$

In vector form

$$\rho \left\{ \frac{\partial \bar{v}}{\partial t} + (\bar{v} \text{grad}) \bar{v} \right\} = \rho \bar{f} + \text{Div} \underline{\underline{\sigma}}, \quad (2.2.7)$$

corresponds with the motion equation (2.2.5), while

$$\rho \frac{\partial^2 \bar{s}}{\partial t^2} = \rho \bar{f} + \text{Div} \underline{\underline{\sigma}} \quad (2.2.8)$$

refers to equation (2.2.6), where Div is the sign of the tensor divergence and the double underline denotes the tensor.

The continuity equation (2.2.4) and equation (2.2.5) are the continuum mechanical formulation of the mass conservation and the impulse thesis respectively, i.e. express general (valid for any continuum) law of nature. However there are 10 scalar unknowns in these four scalar equations (assuming the mass forces f_i as knowns). Thus equations derived from natural basic law are significantly underdetermined, so unambiguous solution can not be existed.

To clearly describe dynamically the movement of the continuum more six equations are required which can be obtained on the basis of restrictive conditions took to the material quality of continuum and its elastic properties. These equations are the material equations wrote to the six independent elements of the stress tensor.

2.3. Material equations

Elastic properties of material continua are very diverse. A general material equation which comprise all of this variety, does not exist. Instead, one should highlight from all elastic properties of the investigated medium the most relevant ones and neglect the other "disturbing" circumstances. This can be expressed differently i.e. we create a model. The most important simple and complex material models built from the simple ones will be described in the followings especially considering the rock mechanics and seismic/acoustic aspects.

2.3.1. Material equation of the perfectly elastic body, stress dependent elastic parameters

Perfectly elastic body means that stresses depend on the deformations dominant at a given space of the continuum in a given time, i.e.

$$\sigma_{ik} = f_{ik}(\varepsilon_{11}, \varepsilon_{22}, \varepsilon_{33}, \varepsilon_{12}, \varepsilon_{13}, \varepsilon_{23}). \quad (2.3.1)$$

The function f_{ik} is generally non-linear. However, very often we deal with small stress change related to small deformations. For example, if an elastic wave propagates in a medium existed in a given stress state, the wave-induced deformation and stress perturbation is very small compared to the characteristics of the original, static load of the medium.

In this case, the function f_{ik} can be approximated by the linear parts of its power series

$$\sigma_{\beta} = \sigma_{\beta}^{(0)} + \sum_{\alpha=1}^6 \left(\frac{\partial f_{\beta}}{\partial \varepsilon_{\alpha}} \right)_{\varepsilon_0} \delta \varepsilon_{\alpha}, \quad (2.3.2)$$

where the notations

$$\sigma_{\beta} = \{\sigma_{11}, \sigma_{22}, \sigma_{33}, \sigma_{12}, \sigma_{13}, \sigma_{23}\}$$

$$\varepsilon_{\alpha} = \{\varepsilon_{11}, \varepsilon_{22}, \varepsilon_{33}, \varepsilon_{12}, \varepsilon_{13}, \varepsilon_{23}\}$$

were introduced. The constants $c_{\alpha\beta} = \left(\frac{\partial f_\beta}{\partial \varepsilon_\alpha} \right)_{\varepsilon_0}$ are named elastic constants which characterize the perfectly elastic body near the undeformed state. Obviously, the series expansion can be performed around any deformation state, when

$$\begin{aligned}\varepsilon &= \varepsilon_\alpha^{(0)} + \delta \varepsilon_\alpha \ , \\ \sigma_\beta &= \sigma_\beta^{(0)} + \delta \sigma_\beta \ .\end{aligned}$$

Then

$$\sigma_\beta^{(0)} + \delta \sigma_\beta = f_\beta \left(\varepsilon_\alpha^{(0)} \right) + \sum_{\alpha=1}^6 \left(\frac{\partial f_\beta}{\partial \varepsilon_\alpha} \right)_{\varepsilon_\alpha^{(0)}} \delta \varepsilon_\alpha \ ,$$

or because of $\sigma_\beta^{(0)} = f_\beta \left(\varepsilon_\alpha^{(0)} \right)$

$$\delta \sigma_\beta = \sum_{\alpha=1}^6 \left(\frac{\partial f_\beta}{\partial \varepsilon_\alpha} \right)_{\varepsilon_\alpha^{(0)}} \delta \varepsilon_\alpha \ . \quad (2.3.3)$$

Small deformations $\delta \varepsilon_\alpha$ superposed to the basic (or equilibrium) deformation are -similarly to (2.3.2) - connected to stress change $\delta \sigma_\beta$ by the equation (2.3.3), but elastic „constants”

$$c_{\alpha\beta} \left(\underline{\varepsilon}^{(0)} \right) = \left(\frac{\partial f_\beta}{\partial \varepsilon_\alpha} \right)_{\varepsilon_\alpha^{(0)}}$$

depend on the basic deformations. If the function $\sigma_\beta = f_\beta \left(\varepsilon_\alpha \right)$ can be inverted, i.e. $\varepsilon_\alpha = g_\alpha \left(\sigma_\beta \right)$ the elastic properties $c_{\alpha\beta} \left(\underline{\sigma} \right)$ depend on stress state. This is supported by the seismic experience that the velocity of elastic waves is a function of in-situ stress state. Since the propagation velocity depends on elastic moduli one can see that the model of the perfectly elastic body can be phenomenological suitable to describe the velocity/pressure relationship through the pressure-dependent moduli. Of course the production of the appropriate materials equation depends on rock type and rock quality.

Since waves mean small deformation, this time the series expansion (2.3.3) provides good approximation. Elastic parameters $c_{\alpha\beta} = \left(\frac{\partial f_\beta}{\partial \varepsilon_\alpha} \right)_0$ in (2.3.3) form a 6x6 matrix. It can be

proved by the help of the energy thesis formulated to continua, this matrix is symmetric. This means that in general case, the elastic properties of the anisotropic continuum can be characterized by 21 independent elastic parameters. The properties of material symmetry can significantly reduce the number of elastic constants. Isotropic continuum can be characterized by two elastic constants. In case of several practical instance, linear approximation (2.3.3) denotes a good approximation but in seismics apart from explosion issues. That material model in which (2.3.3) is valid for not only small deformations, is called the model of linearly elastic body. In small deformation interval the model of perfectly elastic body transforms to linearly elastic body.

2.3.2. Material and motion equation of Hooke-body

The phenomenological description of anisotropy is very important in rock physics and seismic too. However, the simplification is reasonable in seismic practice the most widely used linearly elastic medium model assumes isotropy. The linearly elastic isotropic body is characterized by only two elastic parameters which can be introduced a number of ways. With thermodynamic considerations the two parameters are the so-called first μ and second λ Lamé coefficients with which the material equation of the linearly elastic isotropic body or Hooke-body can be written as

$$\sigma_{ik} = 2\mu \varepsilon_{ik} + \lambda \Theta \delta_{ik}. \quad (2.3.4)$$

Hence to the main diagonal of the stress tensor one can obtain the equation

$$\sigma_{qq} = 3K\Theta, \quad (2.3.5)$$

where $K = \lambda + \frac{2}{3}\mu$ is the compression modulus.

Introducing the stress spherical tensor

$$T_{ik}^{(0)} = \frac{1}{3} \sigma_{qq} \delta_{ik},$$

on the basis of (2.3.5) its relationship with the deformation spherical tensor is

$$T_{ik}^{(0)} = 3K E_{ik}^{(0)}. \quad (2.3.6)$$

The stress deviatoric tensor $T_{ik} = \sigma_{ik} - T_{ik}^{(0)}$ after (2.3.4) is

$$T_{ik} = 2\mu E_{ik}. \quad (2.3.7)$$

The material characteristic parameters μ and λ are generally depend on temperature too.

In engineer life instead of Lamé coefficients the Young's modulus E and Poisson's number m are often used. In case of uniaxial load (e.g. a thin long rod clamped at one end, its other end is pulled) if x_1 is axial, the tensile is

$$\sigma_{11} = E \varepsilon_{11}, \quad (2.3.8)$$

so the Young's modulus E can be determined directly. In the plane perpendicular to the tension the deformations $\varepsilon_{22}, \varepsilon_{33}$ have opposite sign and proportional to the relative expansion ε_{11}

$$\varepsilon_{22} = \varepsilon_{33} = -\frac{1}{m} \varepsilon_{11},$$

where m is the Poisson's number. The relative volume change is

$$\Theta = \varepsilon_{11} + \varepsilon_{22} + \varepsilon_{33} = \frac{m-2}{m} \varepsilon_{11}. \quad (2.3.9)$$

Since in case of $\varepsilon_{11} > 0$ (stretching) the volume can not decrease ($\Theta \geq 0$) so from (2.3.9) $m \geq 2$. The equality refers to incompressible materials ($\Theta = 0$) (e.g. static load in fluid).

To look for the relationship of parameters μ, λ and E, m write the expression of Θ (2.3.9) to (2.3.4). At uniaxial load

$$\sigma_{11} = \left(2\mu + \lambda \frac{m-2}{m} \right) \varepsilon_{11}, \quad (2.3.10)$$

on the other hand because of $\sigma_{qq} = \sigma_{11}$ (since there is only one stress component exists)

$$\sigma_{11} = (3\lambda + 2\mu) \frac{m-2}{m} \varepsilon_{11}. \quad (2.3.11)$$

By comparing the equations (2.3.10) and (2.3.11), as well as (2.3.8)

$$m = 2 \left(1 + \frac{\mu}{\lambda} \right),$$

$$E = \frac{\mu}{\lambda + \mu} (3\lambda + 2\mu)$$

or

$$\mu = \frac{m}{2(m+1)} E ,$$

$$\lambda = \frac{m}{(m+1)(m-2)} E .$$

One can obtain the motion equation of the linearly elastic isotropic body if one substitutes the material equation (2.3.4) to the general motion equation (2.2.6). By forming the divergence of the stress tensor (2.3.4) in case of homogeneous medium (μ and λ are independent from location)

$$\frac{\partial \sigma_{ik}}{\partial x_k} = \mu \frac{\partial^2 u_i}{\partial x_k \partial x_k} + \mu \frac{\partial^2 u_k}{\partial x_k \partial x_i} + \lambda \frac{\partial \Theta}{\partial x_k} \delta_{ik} ,$$

where the definition (2.1.7) of the deformation tensor was used and one must sum for the same indexes. Since

$$\frac{\partial^2 u_k}{\partial x_k \partial x_i} = \frac{\partial}{\partial x_i} \frac{\partial u_k}{\partial x_k} = \frac{\partial \Theta}{\partial x_i}$$

and

$$\frac{\partial \Theta}{\partial x_k} \delta_{ik} = \frac{\partial \Theta}{\partial x_i} ,$$

the motion equation can be written as

$$\rho \frac{\partial^2 u_i}{\partial t^2} = \rho f_i + \mu \Delta u_i + (\lambda + \mu) \frac{\partial \Theta}{\partial x_i} , \quad (2.3.12)$$

in vectorial form by using (2.1.10)

$$\rho \frac{\partial^2 \vec{s}}{\partial t^2} = \rho \vec{f} + \mu \Delta \vec{s} + (\lambda + \mu) \text{grad div } \vec{s} . \quad (2.3.13)$$

This equation alias the Lamé equation is the motion equation of the linearly elastic homogeneous body (Hooke-body). Mathematically (2.3.13) is an inhomogeneous, second-order non-linear coupled partial differential equation system. To obtain its unambiguous solution initial and boundary conditions are necessary. Setting the initial value problem means that we require the displacement $\vec{s}(\vec{r}, 0)$ and velocity $\vec{v}(\vec{r}, 0)$ at each point of the tested V volume in $t = 0$.

Boundary conditions require the displacement $\bar{s}(\bar{r}^*, t)$ and the value of the directional (normal) derivative $\frac{\partial \bar{s}}{\partial \bar{n}}$ at any t time in \bar{r}^* points of the surface A bounding volume V .

In case of inhomogeneous linearly elastic isotropic body the „Lame coefficients” depend on space: $\mu = \mu(x_1, x_2, x_3)$, $\lambda = \lambda(x_1, x_2, x_3)$. So the divergence of the stress tensor (2.3.4) can be written in the form

$$\frac{\partial \sigma_{ik}}{\partial x_k} = \mu \Delta u_i + (\lambda + \mu) \frac{\partial}{\partial x_i} \text{div } \bar{s} + \frac{\partial \mu}{\partial x_k} \frac{\partial u_i}{\partial x_k} + \frac{\partial \mu}{\partial x_k} \frac{\partial u_k}{\partial x_i} + \frac{\partial \lambda}{\partial x_i} \text{div } \bar{s} .$$

With which the motion equation is

$$\rho \frac{\partial^2 u_i}{\partial t^2} = \rho f_i + \mu \Delta u_i + (\lambda + \mu) \frac{\partial}{\partial x_i} \text{div } \bar{s} + \frac{\partial \mu}{\partial x_k} \frac{\partial u_i}{\partial x_k} + \frac{\partial \mu}{\partial x_k} \frac{\partial u_k}{\partial x_i} + \frac{\partial \lambda}{\partial x_i} \text{div } \bar{s}$$

or in vectorial form

$$\rho \frac{\partial^2 \bar{s}}{\partial t^2} = \rho \bar{f} + \mu \Delta \bar{s} + (\lambda + \mu) \text{grad div } \bar{s} + 2(\text{grad } \mu \text{ grad}) \bar{s} + [\text{grad } \mu, \text{rot } \bar{s}] + \text{grad } \lambda \text{ div } \bar{s}$$

where $[\text{grad } \mu, \text{rot } \bar{s}]$ denotes vectorial multiplication.

2.3.3. Fluid mechanical material models and their motion equations

Fenomenological definition of fluids is based on the experience that the smaller the tangential (shear) stresses occurring in fluids are the slower the deformation is. By extrapolating this observation we consider that continuum as fluid, in which shear stresses do not occur in repose state, i.e. elements outside the main diagonal of the stress tensor are disappeared in every coordinate system. In isotropic fluids, elements in the main diagonal are equal, i.e. the stress tensor in repose state is

$$\sigma_{ik} = -p \delta_{ik} ,$$

where p is the scalar pressure.

Material and motion equation of ideal fluid (Pascal's body)

We call that fluid ideal in which shear stresses during motion do not occur, i.e. the stress tensor of the ideal fluid for any deformation is

$$\sigma_{ik} = -p \delta_{ik} . \tag{2.3.14}$$

Since then

$$T_{ik}^{(0)} = \sigma_{ik} ,$$

the stress tensor of the ideal fluid is a spherical tensor. This is another formulation of the well known - from fluid mechanics - Pascal's law, therefore the ideal fluid called otherwise Pascal's body.

Equation (2.3.14) only makes constraint to the format of the stress tensor, but it is not a material equation. The material equation usually connects the stresses with kinematic characteristics. In contrary in fluid mechanics the pressure is investigated in density and temperature dependence. For example if pressure depends on only density

$$p = p(\rho) ,$$

we talk about barotropic fluid.

Equation (2.3.14) is valid in case of gases too. The state equation of ideal gases can be written as

$$\frac{p}{\rho T} = R ,$$

where R is the gas constant and T is the absolute temperature. The state equation is simpler in case of special change of state. E.g. at isothermal processes

$$\frac{p}{\rho^\kappa} = \textit{konstans} ,$$

while in case of adiabatic change of state

$$\frac{p}{\rho^\kappa} = \textit{konstans} ,$$

where $\kappa = \frac{c_p}{c_v}$, c_p is the specific heat measured at constant pressure as well as c_v is at constant

volume, respectively. Based on (2.2.5) and (2.3.14) the motion equation of the ideal fluid is

$$\rho \left(\frac{\partial v_i}{\partial t} + \bar{v} \textit{grad} v_i \right) = \rho f_i - \frac{\partial p}{\partial x_i}$$

or in vectorial form

$$\rho \left\{ \frac{\partial \bar{v}}{\partial t} + (\bar{v} \text{ grad}) \bar{v} \right\} = \rho \bar{f} - \text{grad } p . \quad (2.3.15)$$

This equation is the so-called Euler-equation.

Material and motion equation of the Newtonian fluid

The ideal fluid model not enables to describe a number of practical problems. It is a general experience that waves absorb in fluids or friction losses occur in fluids during flowing. To explain these phenomena an improved fluid model is required.

At the phenomenological definition of fluids we highlighted that shear stresses are the smaller the slower the deformation is. This means that stresses in fluid originated from friction depend on the swiftness of the deformations, the deformation velocity tensor

$$\dot{\varepsilon}_{ik} = \frac{\partial \varepsilon_{ik}}{\partial t} = \frac{1}{2} \left(\frac{\partial v_i}{\partial x_k} + \frac{\partial v_k}{\partial x_i} \right)$$

i.e.

$$\sigma'_{ik} = f_{ik} \left(\dot{\varepsilon}_{11}, \dot{\varepsilon}_{22}, \dot{\varepsilon}_{33}, \dot{\varepsilon}_{12}, \dot{\varepsilon}_{13}, \dot{\varepsilon}_{23} \right) .$$

In terms of geophysical applications only the isotropic fluids have significance which show linear dependence in deformation velocities. Then (because of the isotropy) writing the tensor $\dot{\varepsilon}_{ik}$ instead of deformations ε_{ik} in the (2.3.4) formula of the tensor σ_{ik} , one obtains the material equation

$$\sigma'_{ik} = 2\eta \dot{\varepsilon}_{ik} + \zeta \dot{\Theta} \delta_{ik} , \quad (2.3.16)$$

where η and ζ are the viscous moduli. This is the material equation of the Newtonian fluids (Newton's body). Introducing the deformation velocity spherical tensor

$$\dot{E}_{ik}^{(0)} = \frac{1}{3} \dot{\Theta} \delta_{ik}$$

and the deformation velocity deviator tensor

$$\dot{E}_{ik} = \dot{\varepsilon}_{ik} - \frac{1}{3} \dot{\Theta} \delta_{ik}$$

equation (2.3.16) can be divided into two tensor equations

$$T_{ik} = 2\eta \dot{E}_{ik}, T_{ik}^{(0)} = 3\zeta_v \dot{E}_{ik}^{(0)}, \quad (2.3.17)$$

where $\zeta_v = \zeta + \frac{2}{3}\eta$ is the so-called bulk viscosity.

In reality, to describe the frictional fluids the material equations of the Pascal's and Newton's body should be combined, i.e. the total stress tensor is

$$\sigma_{ik} = -p \delta_{ik} + 2\eta \dot{\varepsilon}_{ik} + \zeta \dot{\Theta} \delta_{ik}.$$

By forming the divergence of the tensor and using (2.3.16) one obtains

$$\frac{\partial \sigma_{ik}}{\partial x_k} = -\frac{\partial p}{\partial x_i} + \eta \frac{\partial^2 v_i}{\partial x_k \partial x_k} + (\eta + \zeta) \frac{\partial}{\partial x_i} \frac{\partial v_l}{\partial x_l},$$

with which the motion equation (2.2.5) can be written as

$$\rho \left(\frac{\partial v_i}{\partial t} + \bar{v} \text{grad} v_i \right) = \rho f_i - \frac{\partial p}{\partial x_i} + \eta \Delta v_i + (\eta + \zeta) \frac{\partial}{\partial x_i} \text{div} \bar{v}, \quad (2.3.18)$$

or in vectorial form

$$\rho \left\{ \frac{\partial \bar{v}}{\partial t} + (\bar{v} \text{grad}) \bar{v} \right\} = \rho \bar{f} - \text{grad} p + \eta \Delta \bar{v} + (\eta + \zeta) \text{grad} \text{div} \bar{v}.$$

This is the motion equation of frictional fluids, i.e. the Navier-Stokes equation.

The Navier-Stokes fluid

Experiences denote that (relative to the sound velocity), at low-velocity flows and low frequency sound waves the bulk viscosity in (2.3.17) can be considered approximately zero. (The measurement of ζ_v is difficult because of this small effect which becomes possible primarily in case of high-frequency ultrasound experiments.) Therefore the Newton-model can be constructed in seismic and rock mechanical applications. It allows us to create a new fluid model in which because of $\zeta_v = 0$

$$\zeta = -\frac{2}{3}\eta, \quad (2.3.19)$$

therefore the stress tensor instead of (2.3.16) is

$$\sigma'_{ik} = 2\eta \left(\dot{\varepsilon}_{ik} - \frac{1}{3} \dot{\Theta} \delta_{ik} \right), \quad (2.3.20)$$

and due to (2.3.20) equation (2.3.17) is

$$T_{ik} = 2\eta \dot{E}_{ik}, T_{ik}^{(0)} = 0. \quad (2.3.21)$$

Equations (2.3.20) or (2.3.21) are the material equation of the so-called Navier-Stokes's body. Due to (2.3.19) the motion equation (2.3.18) can be written as

$$\rho \left(\frac{\partial v_i}{\partial t} + \bar{v} \text{grad } v_i \right) = \rho f_i - \frac{\partial p}{\partial x_i} + \eta \Delta v_i + \frac{\eta}{3} \frac{\partial}{\partial x_i} \text{div } \bar{v},$$

or in vectorial form

$$\rho \left\{ \frac{\partial \bar{v}}{\partial t} + (\bar{v} \text{grad}) \bar{v} \right\} = \rho \bar{f} - \text{grad } p + \eta \Delta \bar{v} + \frac{\eta}{3} \text{grad div } \bar{v}.$$

2.3.4. Rheological material models and their motion equations

The material equations of Hooke's body (2.3.4) and Newton's body (2.3.16) in elastic aspect describes two important limit cases of isotropic material continua: the limit case of stresses depends on only the deformations (2.3.4), as well as depends on (linearly) only the deformation velocity (2.3.16) respectively. In reality, the stress tensor of the medium (in more or less scale) depends on the deformations and the deformation velocities

$$\sigma_{ik} = f_{ik} \left(\underline{\underline{\varepsilon}}, \underline{\underline{\dot{\varepsilon}}} \right),$$

or otherwise the material equation can be written in the general form of

$$F \left(\sigma_{ik}, \varepsilon_{ik}, \dot{\varepsilon}_{ik} \right) = 0. \quad (2.3.22)$$

In many cases, this material equation can be produced according to the equations (2.3.4) and (2.3.16) or (2.3.4) and (2.3.20), in other words the material model describing the elastic properties of the medium can be built from Hooke's and Newton's body or Navier-Stokes's body. In this case we are talking about a complex material model. Often, the stress change velocity tensor $\dot{\sigma}_{ik}$ plays a role in the material equation, i.e. the material equation is

$$F \left(\sigma_{ik}, \dot{\sigma}_{ik}, \varepsilon_{ik}, \dot{\varepsilon}_{ik} \right) = 0. \quad (2.3.23)$$

The function F is usually linear appearing in (2.3.22), (2.3.23), the so-called rheological equations. Then the stress tensor is the linear expression of tensors $\varepsilon_{ik}, \dot{\varepsilon}_{ik}$ and σ_{ik} to which one will see some examples in the followings.

The material and motion equations of the Kelvin-Voigt's body

The Kelvin-Voigt model shows the simplest combination of the Hooke's and Newton's body. Figure 2.1. illustrates the model.

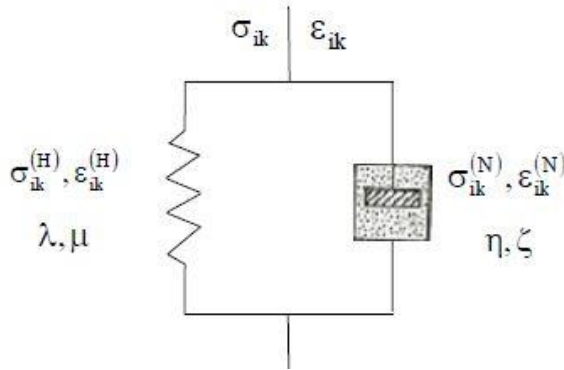


Figure 2.1.: Model of the Kelvin-Voigt's body

The spring models the Hooke's body, while the perforated piston moving in the viscous fluid-filled cylinder models the Newton's body. In case of one-dimensional motions it is obvious that the displacements on the two body parts are equal, while the sum of the forces arose in the two branches of the model are equal to the forces affected to the model. This simple criterion can be generalized as follows

$$\varepsilon_{ik} = \varepsilon_{ik}^{(H)} = \varepsilon_{ik}^{(N)} \quad (2.3.24)$$

$$\sigma_{ik} = \sigma_{ik}^{(H)} + \sigma_{ik}^{(N)}. \quad (2.3.25)$$

By using the material equations (2.3.4) and (2.3.17), (2.3.24), (2.3.25) provides the following result

$$\sigma_{ik} = 2\mu\varepsilon_{ik} + \lambda\Theta\delta_{ik} + 2\eta\dot{\varepsilon}_{ik} + \zeta\dot{\Theta}\delta_{ik} \quad (2.3.26)$$

which is the material equation of the Kelvin-Voigt's body. Based on (2.3.26) to the stress deviator tensor one obtains

$$T_{ik} = 2\mu E_{ik} + 2\eta \dot{E}_{ik} \quad (2.3.27)$$

or by introducing the so-called retardation time

$$g = \frac{\eta}{\mu}$$

one gets the equation

$$T_{ik} = \left\{ I + g \frac{\partial}{\partial t} \right\} 2\mu E_{ik} . \quad (2.3.28)$$

One can see that in case of slow processes this material equation pass through the material equation of the Hokke's body. If t_0 is the characteristic time of the process then $\frac{E_{ik}}{t_0}$ gives the order of magnitude of the derivative. In case of slow processes

$$\frac{g}{t_0} \ll 1$$

then indeed $T_{ik} = 2\mu E_{ik}$. In case of fast processes

$$\frac{g}{t_0} \gg 1 ,$$

then the equation (2.3.28) can be approximated by

$$T_{ik} = 2\mu g \dot{E}_{ik}$$

which is the deviator equation of the Newton's body due to $2\mu g = 2\eta$.

The equation of the spherical tensors are

$$T_{ik}^{(0)} = 3K E_{ik}^{(0)} + 3\zeta_v \dot{E}_{ik}^{(0)} , \quad (2.3.29)$$

where $K = \lambda + \frac{2}{3}\mu$, $\zeta_v = \zeta + \frac{2}{3}\eta$.

If the Navier-Stokes's body describes the viscous forces instead of Newton's body, the deviator equation remains unchanged but for the equation of the spherical tensor instead of (2.3.29) one obtains

$$T_{ik}^{(0)} = 3K E_{ik}^{(0)} . \quad (2.3.30)$$

This approximation is adequate for the description of rock mechanical and seismic phenomena in many cases.

Solve the differential equation (2.3.28) to analyze the properties of the Kelvin-Voigt's body. Introducing the notation $G_{ik} = T_{ik} - 2\mu E_{ik}$ to (2.3.28) one gets the equation

$$\dot{G}_{ik} + \frac{I}{g} G_{ik} = \dot{T}_{ik} . \quad (2.3.31)$$

We look for the solution by the method of varying constants in the following form

$$G_{ik} = c_{ik}(t) e^{-\frac{t}{g}} . \quad (2.3.32)$$

To the function c_{ik} from (2.3.31) one obtains the equation

$$\dot{c}_{ik} = e^{\frac{t}{g}} \dot{T}_{ik}(t)$$

from where

$$c_{ik} = \int_0^t e^{\frac{t'}{g}} \dot{T}_{ik}(t') dt' + K_{ik} ,$$

where K_{ik} is constant. Thus based on (2.3.32) the solution of (2.3.31) is

$$T_{ik} - 2\mu E_{ik} = e^{-\frac{t}{g}} \left(K_{ik} + \int_0^t e^{\frac{t'}{g}} \dot{T}_{ik}(t') dt' \right) . \quad (2.3.33)$$

The initial condition in $t=0$ is specified in the form of $T_{ik} = T_{ik}(0), E_{ik} = 0$, therefore

$K_{ik} = T_{ik}(0)$, so from (2.3.33) one gets the equation

$$E_{ik} = \frac{I}{2\mu} \left\{ T_{ik} - T_{ik}(0) e^{-\frac{t}{g}} - \int_0^t e^{-\frac{t-t'}{g}} \dot{T}_{ik} dt' \right\} . \quad (2.3.34)$$

One can see that the deformations E_{ik} are differ from the value $\frac{I}{2\mu}T_{ik}$ according to the Hooke's body and show explicit time dependence. If e.g. we consider that special case when we load the Kelvin-Voigt's body by constant stress ($\dot{T}_{ik} = 0$), then due to $T_{ik} = T_{ik}(0)$

$$E_{ik} = \frac{I}{2\mu}T_{ik}(0)\left(1 - e^{-\frac{t}{\mathcal{G}}}\right),$$

i.e. deformations approximate asymptotically the value $E_{ik}^{(\infty)} = \frac{I}{2\mu}T_{ik}(0)$ got based on the Hooke's model. Parameter \mathcal{G} clarifies the velocity of this approximation. This is that time during which E_{ik} puts the $\left(1 - \frac{1}{e}\right)$ -fold of the asymptotic value on.

Since the deformation of the Kelvin-Voigt's body reaches the value belongs to the Hooke's body only delayed (retarded), the rheological parameter \mathcal{G} is called retardation time. The rock mechanical process described above and illustrated in Figure 2.2. is called creep.

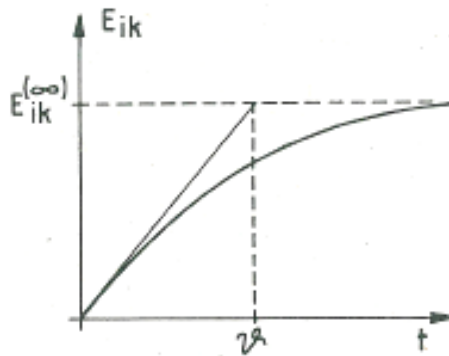


Figure 2.2.: The phenomenon of creep and the geometric meaning of parameter \mathcal{G}

Returning to the general equation (3.2.34), by partial integration one obtains from it an initial condition independent formula

$$E_{ik} = \frac{I}{2\eta_0} \int_0^t e^{-\frac{t-t'}{\mathcal{G}}} T_{ik}(t') dt'.$$

Herewith – contrasting the Kelvin-Voigt's body with the Hooke's body - an example can be seen to that the deformations in the body in given time t depend on not the value of the stresses in the same time but the stresses took in the previous interval $(0, t)$.

One obtains the motion equation of the Kelvin-Voigt's body by substituting the material equation (2.3.26) to (2.2.6).

$$\rho \frac{\partial^2 u_i}{\partial t^2} = \rho f_i + \mu \Delta u_i + (\lambda + \mu) \frac{\partial}{\partial x_i} \operatorname{div} \bar{s} + \eta \Delta v_i + (\eta + \zeta) \frac{\partial}{\partial x_i} \operatorname{div} \bar{v}, \quad (2.3.35)$$

or in vectorial form

$$\rho \frac{\partial^2 \bar{s}}{\partial t^2} = \rho \bar{f} + \mu \Delta \bar{s} + (\lambda + \mu) \operatorname{grad} \operatorname{div} \bar{s} + \eta \Delta \bar{v} + (\eta + \zeta) \operatorname{grad} \operatorname{div} \bar{v}. \quad (2.3.36)$$

The material equation of the Maxwell body

As it was presented, the Kelvin-Voigt body built up from the Hooke and Newton bodies behaves as linearly elastic body in case of static border-line case, and as viscous fluid in case of fast processes. Another material model can be built up from the Hooke and Newton bodies as well, which acts like fluid in slow processes and as elastic solid continuum in fast ones. This is the model of the Maxwell body illustrated sematically in Figure 2.3.

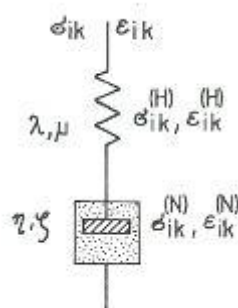


Figure 2.3.: The model of the Maxwell body

Thinking about the one dimensional motions based on the figure it can be seen that the same forces arise in the two elements of the model and the sum of the displacements of the two elements is equal to the total displacement. Generalized this, the equations

$$\begin{aligned}\sigma_{ik} &= \sigma_{ik}^{(H)} = \sigma_{ik}^{(N)} \\ \varepsilon_{ik} &= \varepsilon_{ik}^{(H)} + \varepsilon_{ik}^{(N)}\end{aligned}\quad (2.3.37)$$

can be used as basic equations in the deduction of the model's material equation. Based on the material equations of the Hooke and Newton bodies

$$\sigma_{ik} = 2\mu \varepsilon_{ik}^{(H)} + \lambda \Theta^{(H)} \delta_{ik} \quad (2.3.38)$$

and

$$\sigma_{ik} = 2\eta \dot{\varepsilon}_{ik}^{(N)} + \zeta \dot{\Theta}^{(N)} \delta_{ik}. \quad (2.3.39)$$

From (2.3.38) the $\sigma_{qq} = (3\lambda + 2\mu) \Theta^{(H)}$, or $\Theta^{(H)} = \frac{\sigma_{qq}}{3\lambda + 2\mu}$. With this the equation

$$\varepsilon_{ik}^{(H)} = \frac{1}{2\mu} \left(\sigma_{ik} - \frac{\lambda}{3\lambda + 2\mu} \sigma_{qq} \delta_{ik} \right)$$

can be obtained for the $\varepsilon_{ik}^{(H)}$ deformations similarly from (2.3.38). However according to (2.3.37)

$$\varepsilon_{ik}^{(N)} = \varepsilon_{ik} - \frac{1}{2\mu} \left(\sigma_{ik} - \frac{\lambda}{3\lambda + 2\mu} \sigma_{qq} \delta_{ik} \right),$$

$$\Theta^{(N)} = \Theta - \frac{\sigma_{qq}}{3\lambda + 2\mu}$$

and so the material equation of the Maxwell body can be written based on (2.3.39) as

$$\sigma_{ik} + \frac{\eta}{\mu} \dot{\sigma}_{ik} = 2\eta \dot{\varepsilon}_{ik} + \left(\zeta \dot{\Theta} + \frac{\eta}{\mu} \frac{\lambda - \zeta \frac{\mu}{\eta}}{3\lambda + 2\mu} \dot{\sigma}_{qq} \right) \delta_{ik}. \quad (2.3.40)$$

For the trace of the tensor the

$$\sigma_{qq} + \frac{3\zeta + 2\eta}{3\lambda + 2\mu} \dot{\sigma}_{qq} = (3\zeta + 2\eta) \dot{\Theta}$$

equation, and so for the sphere tensors the

$$T_{ik}^{(o)} + \tau_o \dot{T}_{ik}^{(o)} = 3\zeta_v \dot{E}_{ik}^{(o)} \quad (2.3.41)$$

equation arise, where

$$\tau_0 = \frac{3\zeta + 2\eta}{3\lambda + 2\mu} = \frac{\zeta_v}{K}$$

is the volumetrical relaxation time.

Constituting the difference of (2.3.40) and (2.3.41) the deviator equation can be deduced

$$T_{ik} + \tau \dot{T}_{ik} = 2\eta \dot{E}_{ik}, \quad (2.3.42)$$

where $\tau = \frac{\eta}{\mu}$ is the relaxation time.

Note that if we use Navier-Stokes body instead of the Newton body in the Maxwell model, then because of $\zeta_v = \zeta - \frac{2}{3}\eta = 0$ from (2.3.41) $T_{ik}^{(0)} = 0$, i.e. $\sigma_{ik} = T_{ik}$, hence the material equation of the Maxwell body can be written as

$$\sigma_{ik} + \tau \dot{\sigma}_{ik} = 2\eta \left(\varepsilon_{ik} - \frac{1}{3} \dot{\Theta} \delta_{ik} \right). \quad (2.3.43)$$

This approximation can often be applied in case of rocks.

For slow processes ($\tau \ll t_0$, t_0 is the characteristic time of the process) the \dot{T}_{ik} derivative can be neglected in the equation (2.3.42). Then we get the $T_{ik} = 2\eta \dot{E}_{ik}$ approximate equation. In case of slow processes the Maxwell body changes to the model of Newtonian fluid. In case of fast processes ($\tau \gg t_0$) $T_{ik} \ll \tau \dot{T}_{ik}$ in equation (2.3.42), so the equation leads to the $\dot{T}_{ik} = 2\mu \dot{E}_{ik}$ or $T_{ik} = 2\mu E_{ik}$ material equation. It means that the Maxwell body acts in this border-line case as a Hooke body.

Looking for the solution of equation (2.3.42) in the form of

$$T_{ik} = c_{ik}(t) e^{-\frac{t}{\tau}}$$

for the $c_{ik}(t)$ function from (2.3.42) the following result can be obtained

$$c_{ik} = 2\mu \int_0^t e^{\frac{t'}{\tau}} \dot{E}_{ik}(t') dt'$$

whereby

$$T_{ik} = 2\mu \int_0^t e^{-\frac{t-t'}{\tau}} \dot{E}_{ik}(t') dt'.$$

It can be seen from the equation – setting the Maxwell body against the Newton body – that by the Maxwell body the stresses at a given t time depend not only on the deformation velocities dominating at t , but all the \dot{E}_{ik} of previous times in the $(0, t)$ interval influence the value of T_{ik} .

A typical property of the Maxwell body can be shown if the solution relating to time stationary deformations of equation (2.3.42) is derived. There the

$$T_{ik} + \tau \dot{T}_{ik} = 0$$

equation gives the result

$$T_{ik} = T_{ik}^0 e^{-\frac{t}{\tau}}$$

(here the upper case 0 does not indicate the sphere tensor, but the value taken at $t = 0$!). The exponential loss of stresses is shown in Figure 2.4.

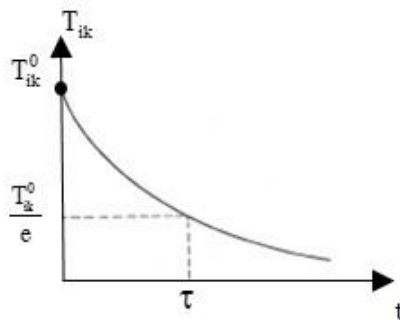


Figure 2.4.: The phenomenon of stress relaxation, the geometrical meaning of the τ parameter

This phenomenon common in rocks is the release or relaxation of stresses. The τ relaxation time is the time during the stresses decrease to the e -th part of the initial T_{ik}^0 value. The Maxwell model is basically a fluid model, no stresses arise in it against static deformations. So it can be used only for explanation of dynamic features during describing rocks.

The material equation of the Poynting-Thomson body

The previously introduced Hooke, Kelvin-Voigt and Maxwell models each took hold of one important side of elastic-rheological features of rocks: the Hooke body the resistance against the static deformations, the Kelvin-Voigt body the creeping, the Maxwell body the stress relaxation. The Poynting-Thomson model or standard body is a rock mechanical model which combines the Hooke and Maxwell bodies as it is shown in Figure 2.5. and it can describe the three phenomena simultaneously. The base equations are

$$\begin{aligned}\varepsilon_{ik} &= \varepsilon_{ik}^{(H)} = \varepsilon_{ik}^{(M)}, \\ \sigma_{ik} &= \sigma_{ik}^{(H)} + \sigma_{ik}^{(M)},\end{aligned}\tag{2.3.44}$$

where $\varepsilon_{ik}^{(M)}, \sigma_{ik}^{(M)}$ are the deformation and stress arising in the Maxwell body.

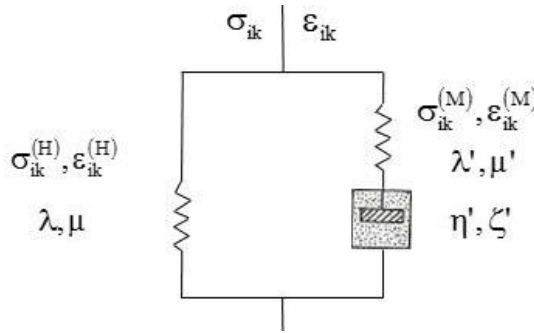


Figure 2.5.: The model of the Poynting-Thomson body

The material equation of the standard body can be obtained after adding the equations (2.3.40) and (2.3.4) together with marking the material properties of the Maxwell body with ' in (2.3.40)

$$\sigma_{ik} = 2 \mu \varepsilon_{ik} + \lambda \Theta \delta_{ik} + 2 \eta' \dot{\varepsilon}_{ik} - \frac{\eta'}{\mu'} \dot{\sigma}_{ik} + \left(\zeta \dot{\Theta} + \frac{\eta' \left(\lambda' - \zeta' \frac{\eta'}{\mu'} \right)}{\mu' (3 \lambda' + 2 \mu')} \dot{\sigma}_{qq} \right) \delta_{ik}.$$

Regarding the equation as sum of a sphere and a deviator tensor the deviator tensor can be derived as

$$T_{ik} = 2 \mu E_{ik} + 2 \eta' \left(I + \frac{\mu}{\mu'} \right) \dot{E}_{ik} - \frac{\eta'}{\mu'} \dot{T}_{ik}, \quad (2.3.45)$$

while the equation of the sphere tensor has the form of

$$T_{ik}^{(0)} = 3 K E_{ik}^{(0)} + 3 \left(\zeta' + \frac{2}{3} \eta' \right) \left(I + \frac{K}{K'} \right) \dot{E}_{ik}^{(0)} - \frac{\zeta' + \frac{2}{3} \eta'}{\lambda' + \frac{2}{3} \mu'} \dot{T}_{ik}^{(0)}, \quad (2.3.46)$$

where $K' = \lambda' + \frac{2}{3} \mu'$.

If we use Navier-Stokes body instead of a Newton body in the Poynting-Thomson model $\zeta_v = \zeta' + \frac{2}{3} \eta' = 0$, equation (2.3.46) has the more simple form

$$T_{ik}^{(0)} = 3 K E_{ik}^{(0)}.$$

This assumption is widely used during the description of many rock mechanical processes.

Introducing the notations

$$\tau = \frac{\eta'}{\mu'}, \quad \mathcal{G} = \frac{\eta'}{\mu'} \left(I + \frac{\mu'}{\mu} \right)$$

$$\tau_0 = \frac{\zeta' + \frac{2}{3} \eta'}{\lambda' + \frac{2}{3} \mu'}, \quad \mathcal{G}_0 = \frac{\zeta' + \frac{2}{3} \eta'}{\lambda' + \frac{2}{3} \mu'} \left(I + \frac{K'}{K} \right)$$

the equations (2.3.45), (2.3.46) can be written in the form

$$\left\{ I + \tau \frac{\partial}{\partial t} \right\} T_{ik} = \left\{ I + \mathcal{G} \frac{\partial}{\partial t} \right\} 2 \mu E_{ik} \quad (2.3.47)$$

$$\left\{ I + \tau_0 \frac{\partial}{\partial t} \right\} T_{ik}^{(0)} = \left\{ I + \mathcal{G}_0 \frac{\partial}{\partial t} \right\} 3 K E_{ik}^{(0)}. \quad (2.3.48)$$

The τ and \mathcal{G} quantities are called the deviatoric relaxation and retardation times respectively, the τ_0 and \mathcal{G}_0 quantities are called volumetric relaxation or rather retardation time. It can be seen, that in the model $\mathcal{G} \geq \tau$ or rather $\mathcal{G}_0 \geq \tau_0$ relations are valid.

The (2.3.47)-(2.3.48) equation system can be substituted with different equations depending on the magnitude of the $\tau, \mathcal{G}, \tau_0$ and \mathcal{G}_0 rheological parameters. Their scope of validity can be given easily by marking the typical duration of rock movements with t_0 .

In case of phenomena varying very slowly in time, i.e.

$$\mathcal{G} \ll t_0, \text{ or rather } \mathcal{G}_0 \ll t_0$$

(2.3.47), (2.3.48) change to the material equation of linearly elastic body

$$T_{ik} = 2 \mu E_{ik}, T_{ik}^{(0)} = 3 K E_{ik}^{(0)}.$$

In case of processes varying faster in time, assuming the $\mathcal{G} \gg \mathcal{G}_0$, or rather the $\tau \gg \tau_0$ relations phenomena can be distinguished, where

$$\mathcal{G} \approx t_0 \text{ and } \mathcal{G}_0 \ll t_0.$$

Then the equations found valid with a good approximation for practical rock mechanical processes can be written (Asszonyi and Richter 1975)

$$\left\{ I + \tau \frac{\partial}{\partial t} \right\} T_{ik} = \left\{ I + \mathcal{G} \frac{\partial}{\partial t} \right\} 2 \mu E_{ik}$$

$$T_{ik}^{(0)} = 3 K E_{ik}^{(0)}.$$

In case of examination of more faster processes

$$\tau \gg t_0,$$

the (2.3.47) changes again to the material equation of linearly elastic body

$$T_{ik} = 2 \mu \frac{\mathcal{G}}{\tau} E_{ik}$$

or in another form

$$T_{ik} = 2(\mu + \mu') E_{ik}.$$

Depending on the relation of rheological parameters the connection between the sphere tensors can be:

- a.) in case of $\tau_0 \ll \tau, \mathcal{G}_0 \ll \mathcal{G}$, if $\mathcal{G}_0 \ll t_0$ the $T_{ik}^{(0)} = 3 K E_{ik}^{(0)}$ eq. can be obtained.
- b.) if $\tau_0 \ll \tau, \mathcal{G}_0 \ll \mathcal{G}$ and $\mathcal{G}_0 \approx t_0$, or rather $\tau_0 \approx t_0$ then beside the linear relationship between the deviatoric tensor, the rheological equation

$$\left\{ I + \tau_0 \frac{\partial}{\partial t} \right\} T_{ik}^{(0)} = \left\{ I + \mathcal{G}_0 \frac{\partial}{\partial t} \right\} 3K E_{ik}^{(0)}$$

can be written between the sphere tensors.

c.) if τ_0 , or rather \mathcal{G}_0 is in the order of magnitude of τ or rather \mathcal{G} , or the process is so fast that the relation

$$\tau_0 \gg t_0$$

is fulfilled, then

$$T_{ik}^{(0)} = 3K \frac{\mathcal{G}_0}{\tau_0} E_{ik}^{(0)},$$

or in other form

$$T_{ik}^{(0)} = 3(K + K') E_{ik}^{(0)},$$

i.e. both in the deviator and in the sphere tensors linear, but with greater elastic moduli $\mu + \mu'$, or rather $K + K'$ compared to the μ, K moduli manifested in slow (quasistatic) processes.

To write the motion equation of a body following the material equation (2.3.47)-(2.3.48), let us solve the equations for T_{ik} , or rather $T_{ik}^{(0)}$! The equation (2.3.47) can be written as

$$T_{ik} - 2\mu E_{ik} + \frac{1}{\tau} (T_{ik} - 2\mu E_{ik}) = \left\{ \frac{\mathcal{G}}{\tau} - I \right\} 2\mu \dot{E}_{ik}.$$

This inhomogeneous equation can be solved in $T_{ik} - 2\mu E_{ik}$ with the variation of constants method. Looking for the solution in the form of

$$T_{ik} - 2\mu E_{ik} = c_{ik}(t) e^{-\frac{t}{\tau}}$$

for the $c_{ik}(t)$ coefficient the

$$c_{ik}(t) = 2\mu \left(\frac{\mathcal{G}}{\tau} - I \right) \int_0^t e^{\frac{t'}{\tau}} \dot{E}_{ik} dt' + K_{ik}$$

equation can be obtained, where K_{ik} denote constants. Using this the solution of the equation (2.3.47) can be written in the following form

$$T_{ik} = 2\mu E_{ik} + 2\mu \left(\frac{g}{\tau} - 1 \right) \int_0^t e^{-\frac{t-t'}{\tau}} \dot{E}_{ik} dt' + K_{ik} e^{-\frac{t}{\tau}}. \quad (2.3.49)$$

Based on the equation it can be pointed out that the stresses arising in a given time in the Poynting-Thomson body depend on all the E_{ik} values in the $(0,t)$ interval.

As we saw the Poynting-Thomson body is a Hooke body characterized by a $\mu + \mu'$ Lamé constant in the case of fast processes. Let us assume that the body is loaded very fast with $T_{ik}^0 = 2(\mu + \mu')E_{ik}^0$ stress (here the upper case 0 does not indicate the sphere tensor, but the value taken at $t = 0$!). Examining a process starting from this initial state at $t = 0$

$$2(\mu + \mu')E_{ik}^0 = 2\mu E_{ik}^0 + K_{ik},$$

from which $K_{ik} = 2\mu' E_{ik}^0$. If the deformations do not vary in the following i.e. $\dot{E}_{ik} = 0$, from (2.3.49)

$$T_{ik} = 2 \left(\mu + \mu' e^{-\frac{t}{\tau}} \right) E_{ik}^0.$$

As it can be seen in Figure 2.6. the stresses decrease from the initial $2(\mu + \mu')E_{ik}^0$ value to the $2\mu E_{ik}^0$ value. This is the relaxation phenomenon in case of the Poynting-Thomson body.

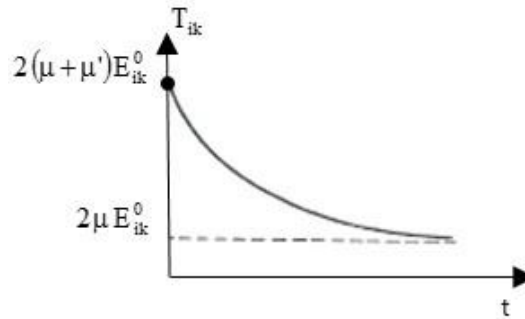


Figure 2.6.: Stress relaxation in case of the Poynting-Thomson body

If we assume that the examined rock mechanical phenomena proceed from the state of permanent equilibrium, we should specify as initial condition that the rock follows the

$$T_{ik} = 2\mu E_{ik}$$

equation of a linearly elastic body at $t = 0$, i.e. $K_{ik} = 0$. In case of such phenomena the general solution of the equation (2.3.47) is

$$T_{ik} = 2 \mu E_{ik} + 2 \mu \left(\frac{\mathcal{G}}{\tau} - I \right) \int_0^t e^{-\frac{t-t'}{\tau}} \dot{E}_{ik} dt'.$$

Since the eq. (2.3.48) corresponds with eq. (2.3.47) structurally, its solution can be written directly:

$$T_{ik}^{(0)} = 3 K E_{ik}^{(0)} + 3 K \left(\frac{\mathcal{G}_0}{\tau_0} - I \right) \int_0^t e^{-\frac{t-t'}{\tau}} \dot{E}_{ik}^{(0)} dt'.$$

Equations (2.3.47), (2.3.48) can be solved for the deformations in a similar manner

$$E_{ik} = \frac{I}{2 \mu} \left\{ T_{ik} - e^{-\frac{t}{\mathcal{G}}} \left[A_{ik} + \left(I - \frac{\tau}{\mathcal{G}} \right) \int_0^t e^{\frac{t'}{\mathcal{G}}} \dot{T}_{ik} dt \right] \right\} \quad (2.3.50)$$

$$E_{ik}^{(0)} = \frac{I}{3 K} \left\{ T_{ik}^{(0)} - e^{-\frac{t}{\mathcal{G}_0}} \left[B_{ik} + \left(I - \frac{\tau_0}{\mathcal{G}_0} \right) \int_0^t e^{-\frac{t'}{\mathcal{G}_0}} \dot{T}_{ik}^{(0)} dt \right] \right\}, \quad (2.3.51)$$

where A_{ik} and B_{ik} are the constants determined by the initial conditions.

If the body is loaded vary fast by a T_{ik}^0 stress the arose deformations can be derived by the formula $E_{ik}^0 = \frac{T_{ik}^0}{2(\mu + \mu')}$, since the standard body approximates the Hooke body in this

process. For the processes starting from this state the relationship $A_{ik} = T_{ik}^0 \frac{\mu'}{\mu + \mu'}$ is valid

based on the initial conditions. If the stresses do not vary later $\left(\dot{T}_{ik} = 0 \right)$ the equation (2.3.50)

can be written as $E_{ik} = \frac{T_{ik}^0}{2 \mu} \left(I - \frac{\mu'}{\mu + \mu'} e^{-\frac{t}{\mathcal{G}}} \right)$.

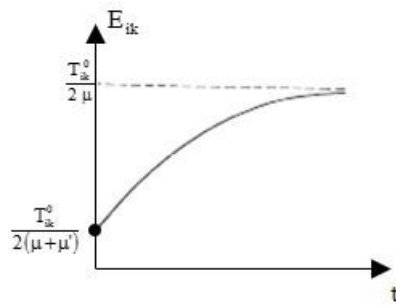


Figure 2.7.: The phenomenon of creeping in the case of the Poynting-Thomson body

As it can be seen in Figure 2.7. the formula describes the increase of deformations from the

$\frac{T_{ik}^0}{2(\mu + \mu')}$ value to the $\frac{T_{ik}^0}{2\mu}$ value. This phenomenon is called creeping. The Poynting-Thomson body can describe both the relaxation and creeping phenomena.

3. Wave propagation in elastic and rheological media

The objective of geophysical investigations is mostly the determination of subsurface structures of the Earth - as material half space - by using surface measurements. For some measurement methods (gravity, magnetic, geoelectric) the impact measured on the surface is integrated in the sense that the quantity measured in a given point reflects theoretically the effect of the whole half space – but at least a space portion to a certain depth. It makes the interpretation much easier if the measured effect yields information from a local area of a determined curve and not from the whole half space. This gives the “simplicity” of the analysis of rocks by elastic waves and its importance as well, because the laws of “beam optic” can be used for the wave propagation in a certain approximation. In the followings the most important features of elastic waves are reviewed with respect to the major material equations discussed previously.

We deal only with low amplitude waves in our investigations. It means that the basic equations are solved with a linear approximation. There is a substantial derivate on the left side of the (2.2.5) general motion equation, where

$$\frac{dv_i}{dt} = \frac{\partial v_i}{\partial t} + \bar{v} \text{ grad } v_i ,$$

where $\bar{v} \text{ grad } v_i$ convective derivative means namely a nonlinear term. Its neglect requires the fulfilment of a simple criteria in case of waves. If T is the periodic time of the wave, λ is the wavelength, A is the amplitude, then the order of magnitude is

$$v_i = \frac{\partial u_i}{\partial t} \approx \frac{A}{T} , \quad \frac{\partial v_i}{\partial t} \approx \frac{A}{T^2}$$

$$\bar{v} \text{ grad } v_i \approx \frac{A}{T} \frac{A}{T\lambda} \approx \frac{A^2}{T^2\lambda} .$$

The convective derivative can be neglected beside the $\frac{\partial v_i}{\partial t}$ local derivative if

$\frac{\partial v_i}{\partial t} \gg \bar{v} \text{ grad } v_i$, i.e. $\frac{A}{T^2} \gg \frac{A^2}{T^2\lambda^2}$, i.e. $A \ll \lambda$. If this criteria is fulfilled, then we can speak about (compared to the wavelength) low amplitude waves. In this case we can write the linear $\frac{\partial v_i}{\partial t}$ derivate instead of $\frac{dv_i}{dt}$.

The assumption of homogeneous medium – especially if it has an infinite dimension – is unsubstantiated in geophysical aspect. We still use this approximation, because the most important properties of the wave space, the connection between the parameters characterizing the waves can be introduced most easily in case of wave propagation in infinite homogeneous medium. We do not have to consider boundary conditions during solving the differential equations in infinite homogeneous space. It is a significant simplification. The so evolving waves are called body waves. (The assumption of infinite spreading is abstraction of course, which means the restriction that the surfaces - maybe existing in the medium - are very far from each other regarding to the wavelength.) In the followings the properties of body waves propagating in infinite homogeneous medium following different material equations are summarized.

3.1. Low amplitude waves in ideal fluid

The motion equation of ideal fluid is given by (2.3.15). The low amplitude wave solution of the equation can be written in the following form

$$\frac{\partial \vec{v}}{\partial t} = \rho \vec{f} - \frac{1}{\rho} \text{grad } p . \quad (3.1)$$

From the point of view of wave theory the importance of \vec{f} mass forces is confined to the determination of equilibrium ρ_0, p_0 distributions. In equilibrium the

$$\rho_0 \vec{f} = \text{grad } p_0$$

statics base equation is valid. For example in case of air this equation determines the density and pressure distributions in the atmosphere of the Earth. This distribution is inhomogeneous, but the inhomogeneity occurs on a very large scale compared to the wave length (for example the wave length of a 100 Hz frequency sound has the order of magnitude of m , which is really small compared to the 10 km order of magnitude of the characteristic changes of the atmosphere). So the medium is locally homogeneous from the point of view of wave propagation, i.e. the equation (3.1) can be solved for homogeneous space. If the wave propagates through distances characterized by inhomogeneity, the changes in accordance with the place of local features (local propagation velocity) should take into account.

As the \vec{f} mass force field has no influence on the wave solution in the order of magnitude of wave length, we can apply the $\vec{f} = 0$ substitution in (3.1), i.e.

$$\frac{\partial \bar{v}}{\partial t} = \frac{-1}{\rho} \text{grad } p.$$

To solve the equation system there is a need for two more equations, for the

$$\frac{\partial \rho}{\partial t} + \text{div} (\rho \bar{v}) = 0$$

continuity equation and for a material equation, for example the $p = p(\rho)$ barotropic equation of state. Assuming that the wave causes the small p', ρ' changes of the p_0, ρ_0 equilibrium features, i.e.

$$p' \ll p_0, \rho' \ll \rho_0$$

the equation system can be linearized. Neglected the product of the p', ρ', \bar{v} quantities or their derivatives the following equations can be obtained

$$\frac{\partial \bar{v}}{\partial t} = \frac{-1}{\rho_0} \text{grad } p' \tag{3.2}$$

$$\frac{\partial \rho'}{\partial t} + \rho_0 \text{div } \bar{v} = 0$$

$$p' = c_h^2 \rho',$$

where $c_h^2 = \left(\frac{\partial p}{\partial \rho} \right)_0$. From the last two equations

$$\frac{1}{\rho_0 c_h^2} \frac{\partial^2 p'}{\partial t^2} = -\text{div} \frac{\partial \bar{v}}{\partial t}, \tag{3.3}$$

the divergence of (3.2) can be written as

$$\text{div} \frac{\partial \bar{v}}{\partial t} = \frac{-1}{\rho_0} \text{div grad } p' = \frac{-1}{\rho_0} \Delta p'.$$

If we compare this equation against (3.3) the

$$\Delta p' - \frac{1}{c_h^2} \frac{\partial^2 p'}{\partial t^2} = 0$$

wave equation can be derived. The following equation can be similarly deduced as well

$$\Delta \bar{v} - \frac{1}{c_h^2} \frac{\partial^2 \bar{v}}{\partial t^2} = 0.$$

The monochromatic plane wave solution of the equations – according to $\Psi = \hat{\Psi}_0 e^{i(\omega t + \vec{k}\vec{r})}$ – can be written in the form of

$$\begin{aligned} p' &= p^* e^{i(\omega t - \vec{k}\vec{r})}, \\ \vec{v} &= \vec{v}^* e^{i(\omega t - \vec{k}\vec{r})}. \end{aligned} \quad (3.4)$$

These functions satisfy the wave equation, but the question is: are they the solution of the motion equation? As we get the equation

$$\text{rot } \vec{v} = 0$$

after forming the rotation of eq. (3.2), it can be seen that the motion equation is fulfilled only in case of $\vec{v} \times \vec{e} = 0$ i.e. the displacement of the wave or rather the velocity of the displacement is parallel to the direction of wave propagation. The (3.4) function describes a longitudinal wave propagating with $c_h = \left(\frac{\partial p}{\partial \rho} \right)_0$ velocity. This solution of the motion equation of ideal fluid (Pascal body) is the sound wave.

3.2. Low amplitude waves in isotropic linearly elastic medium

The motion equation of the linearly elastic isotropic homogeneous medium is given by (2.3.13). As the $\rho \vec{f}$ mass forces can be neglected during the analysis of the wave solution, the motion equation can be written in the following form

$$\rho \frac{\partial^2 \vec{s}}{\partial t^2} = \mu \Delta \vec{s} + (\lambda + \mu) \text{grad div } \vec{s} . \quad (3.5)$$

The \vec{s} vector space, which gives the displacement field, can always be decomposed into the sum of a source-free and a swirl-free vector space

$$\vec{s} = \vec{s}_i + \vec{s}_r, \quad (3.6)$$

where

$$\text{div } \vec{s}_i = 0 \quad (3.7)$$

$$\text{rot } \vec{s}_r = 0 . \quad (3.8)$$

Using the identity

$$\text{rot rot } \vec{s}_i = \text{grad div } \vec{s}_i - \Delta \vec{s}_i$$

for the \bar{s}_l vector space the following relationship can be written

$$\text{grad div } \bar{s}_l = \Delta \bar{s}_l .$$

Based on this equation the

$$\left\{ \rho \frac{\partial^2 \bar{s}_l}{\partial t^2} - \mu \Delta \bar{s}_l \right\} + \left\{ \rho \frac{\partial^2 \bar{s}_l}{\partial t^2} - (\lambda + 2\mu) \Delta \bar{s}_l \right\} = 0 \quad (3.9)$$

formula can be derived by using (3.5). As the order of the partial derivation is interchangeable,

$$\text{div} \left\{ \rho \frac{\partial^2 \bar{s}_l}{\partial t^2} - \mu \Delta \bar{s}_l \right\} = 0$$

ensues from (3.5), i.e. the first term on the left side of (3.9) is source-free as well. It can be seen similarly that the second term in the brackets is swirl-free. As the sum of a source-free and a swirl-free vector spaces can be zero only if the two vector spaces are zeros separately, from (3.9) the

$$\Delta \bar{s}_l - \frac{1}{\beta^2} \frac{\partial^2 \bar{s}_l}{\partial t^2} = 0 \quad (3.10)$$

and the

$$\Delta \bar{s}_l - \frac{1}{\alpha^2} \frac{\partial^2 \bar{s}_l}{\partial t^2} = 0 \quad (3.11)$$

equations can be deduced, where

$$\beta = \sqrt{\frac{\mu}{\rho}}, \quad \alpha = \sqrt{\frac{\lambda + 2\mu}{\rho}} . \quad (3.12)$$

Thus the motion equation gives a separated wave equations each for the source-free \bar{s}_l and the swirl-free \bar{s}_l vector spaces.

The displacement vector potential can be introduced based on (3.7) with the equation

$$\bar{s}_l = \text{rot } \bar{\Psi} , \quad (3.13)$$

while (3.8) can be satisfied trivially if the \bar{s}_l vector space is written as the gradient of the φ scalar displacement potential

$$\bar{s}_l = \text{grad } \varphi . \quad (3.14)$$

The displacement field can be written as

$$\vec{s} = \text{grad } \varphi + \text{rot } \vec{\Psi}$$

based on (3.6), from (3.9) the equation

$$\text{rot} \left\{ \rho \frac{\partial^2 \vec{\Psi}}{\partial t^2} - \mu \Delta \vec{\Psi} \right\} + \text{grad} \left\{ \rho \frac{\partial^2 \varphi}{\partial t^2} - (\lambda + 2\mu) \Delta \varphi \right\} = 0$$

can be derived. It is again a sum of a source- and a swirl-free vector space, therefore the

$$\Delta \vec{\Psi} - \frac{1}{\beta^2} \frac{\partial^2 \vec{\Psi}}{\partial t^2} = 0 \quad (3.15)$$

and the

$$\Delta \varphi - \frac{1}{\alpha^2} \frac{\partial^2 \varphi}{\partial t^2} = 0 \quad (3.16)$$

equations must be met, where α and β are given by (3.12). The vector and scalar displacement potentials satisfy the (3.15), (3.16) wave equations. These equations as well as the equations (3.10) and (3.11) written for the displacements show that two types of body waves can arise in the linearly elastic homogeneous isotropic medium. Based on $\Psi = \Psi_0 e^{i(\omega t - \vec{k}\vec{r} - \varphi)}$ the monochromatic plane wave solution of eq. (3.10) can be written as

$$\vec{s}_t = \vec{s}_t^{(0)} e^{i(\omega t - k_t \vec{e}\vec{r})}, \quad (3.17)$$

where

$$k_t = \frac{\omega}{\beta}. \quad (3.18)$$

The \vec{s}_t vector space satisfies the (3.7) auxiliary condition, therefore the

$$\text{div } \vec{s}_t = -ik_t \vec{s}_t \vec{e} = 0$$

equation should be fulfilled as well, whereof $\vec{s}_t \perp \vec{e}$. The (3.17) describes a transverse wave propagating with β velocity. Since $\Theta = \text{div } \vec{s}_t = 0$, these waves do not result in volume changes.

The monochromatic plane wave solution of (3.11) has the form of

$$\vec{s}_t = \vec{s}_t^{(0)} e^{i(\omega t - k_t \vec{e}\vec{r})}, \quad (3.19)$$

where

$$k_l = \frac{\omega}{\alpha} . \quad (3.20)$$

The \bar{s}_l vector space satisfies the (3.8) auxiliary condition, thus

$$\text{rot } \bar{s}_l = -ik_l \bar{e} \times \bar{s}_l = 0 .$$

This criteria is fulfilled if the directions of displacement and the propagation are parallel. The (3.19) describes a longitudinal wave propagating with α velocity. It can be seen from eq. (3.12) that the latter one in the two types of waves propagating in the Hooke medium is faster

$$\alpha \geq \sqrt{2} \beta .$$

In comparison of the longitudinal and transverse waves originating from a common source the longitudinal waves arrive first to the observation point.

3.3. Low amplitude waves in viscous fluid

After linearization and neglecting the mass forces the (2.3.18) Navier-Stokes equation can be written as

$$\rho_0 \frac{\partial \bar{v}}{\partial t} = -\text{grad } p' + \eta \Delta \bar{v} + (\eta + \zeta) \text{grad } \text{div } \bar{v} . \quad (3.21)$$

Let us stipulate the $\text{rot } \bar{v} = 0$ auxiliary condition and let us form the divergence of the equation! Then with the commutation of the partial derivatives

$$\rho_0 \frac{\partial}{\partial t} \text{div } \bar{v} = -\Delta p' + (\zeta + 2\eta) \Delta \text{div } \bar{v} . \quad (3.22)$$

Based on the linearized continuity equation

$$\text{div } \bar{v} = -\frac{1}{\rho_0} \frac{\partial \rho'}{\partial t} ,$$

from the linearized barotropic equation the

$$p' = c_h^2 \rho'$$

equation can be deduced, with which

$$\text{div } \bar{v} = -\frac{1}{\rho_0 c_h^2} \frac{\partial p'}{\partial t} .$$

Substituting this equation into (3.22)

$$\Delta p' - \frac{I}{c_h^2} \frac{\partial^2 p'}{\partial t^2} - \mathcal{G} \Delta \frac{\partial p'}{\partial t} = 0 ,$$

where $\mathcal{G} = \frac{\zeta + 2\eta}{\rho_0 c_h^2}$. In search of the monochromatic plane wave solution of the equation in the form of

$$p' = p^* e^{i(\omega t - k \bar{e} \bar{r})} ,$$

the following complex dispersion relation can be derived

$$-k^2 (I + i \omega \mathcal{G}) + \frac{\omega^2}{c_h^2} = 0 ,$$

from which

$$k^2 = \frac{\omega^2}{c_h^2} \frac{I - i \omega \mathcal{G}}{I + \omega^2 \mathcal{G}^2} . \quad (3.23)$$

The complex wave number can be written in the form of

$$k = b - i a ,$$

where

$$b = \frac{\omega}{c_h} \sqrt{\frac{I + \sqrt{I + \omega^2 \mathcal{G}^2}}{2(I + \omega^2 \mathcal{G}^2)}} \quad (3.24)$$

$$a = \frac{\omega}{c_h} \sqrt{\frac{-I + \sqrt{I + \omega^2 \mathcal{G}^2}}{2(I + \omega^2 \mathcal{G}^2)}}$$

based on (3.23). (3.25)

In case of water the viscosity is $\eta = 0.01 [Ns/m^2]$, $c_h = 1440 [m/s]$, $\rho_0 = 10^3 [kg/m^3]$. With these data $\mathcal{G} \approx 3.10^{-10} [s]$, i.e. for the frequency $f \ll 5.10^8 [Hz]$

$$\omega \mathcal{G} \ll 1 .$$

This inequality is satisfied in seismic, acoustic and ultrasonic frequencies as well, therefore we can apply series expansion in (3.24), (3.25):

$$b = \frac{\omega}{c_h}$$

$$a = \frac{\omega^2 \mathcal{G}}{2 c_h} = \frac{\omega^2 (\zeta + 2\eta)}{2 \rho_0 c_h^3} .$$

With these

$$p' = p^* e^{i(\omega t - k \bar{e} \bar{r})} = p^* e^{-a \bar{e} \bar{r}} e^{i(\omega t - b \bar{e} \bar{r})} .$$

The longitudinal wave propagates with sound velocity of $\frac{\omega}{b} = c_h$ in viscous fluid and it attenuates with an absorption coefficient of $a = \frac{\omega^2 \mathcal{G}}{2 c_h}$, the attenuation coefficient is proportional

to the square of the frequency. The absorption coefficient is $a \approx 4 \cdot 10^{-4} [1/m]$ in water at a frequency of $f = 10^4 [Hz]$, i.e. the penetration depth of the wave is $d = 1/a \approx 2.5 [km]$. The attenuation is weak: $a < b$, or otherwise the wave length is much smaller than the penetration depth.

The transverse wave solution can be obtained with the $div \bar{v} = 0$ auxiliary condition based on the equations (3.21) and (3.23)

$$\rho_0 \frac{\partial \bar{v}}{\partial t} = \eta \Delta \bar{v} ,$$

which solution is searched in the form of

$$\bar{v} = \bar{v}^* e^{i(\omega t - k \bar{e} \bar{r})} ,$$

and the

$$k^2 = -\frac{i \omega \rho}{\eta}$$

dispersive equation can be deduced. For the complex wave number the following equation can be written

$$k = \sqrt{\frac{\rho \omega}{2\eta}} (1 - i) ,$$

so the real wave number is $b = \sqrt{\frac{\rho \omega}{2\eta}}$, the absorption coefficient is $a = \sqrt{\frac{\rho \omega}{2\eta}}$. The phase

velocity of the wave $v_f = \frac{\omega}{b} = \sqrt{\frac{2\eta \omega}{\rho}}$ is frequency dependent, the wave is dispersive. So

transverse waves can be created in viscous fluid. But these attenuate very strong ($a=b$). The penetration depth is

$$d = \frac{1}{a} = \sqrt{\frac{2\eta}{\rho \omega}} .$$

For example for a wave with a frequency of $f = 10^4$ [Hz] it is $d = 1.7 \cdot 10^{-5}$ [m], which is $\approx 10^8$ times smaller than for a longitudinal wave with the same frequency. Therefore it can be considered in seismic applications that the transverse waves play no role in water.

3.4. Low amplitude waves in Kelvin-Voigt medium

The motion equation of the Kelvin-Voigt body can be written in the form of

$$\rho \frac{\partial^2 \bar{s}}{\partial t^2} = \mu \Delta \bar{s} + (\lambda + \mu) \text{grad div } \bar{s} + \eta \Delta \bar{v} + (\eta + \zeta) \text{grad div } \bar{v}$$

based on (2.3.35) after neglecting the mass forces. In search of the wave solution with the $\text{div } \bar{s} = 0, \text{div } \bar{v} = 0$ auxiliary condition (transverse wave), then the

$$\rho \frac{\partial^2 \bar{s}}{\partial t^2} = \mu \Delta \bar{s} + \eta \Delta \bar{v} \tag{3.26}$$

equation can be derived, which monochromatic plane wave solution has the form of

$$\bar{s}_i = \bar{s}_i^* e^{i(\omega t - k_i \bar{e} \bar{r})} .$$

After substituting it into (3.26) a dispersion relation similar to (3.23) can be obtained

$$k_i^2 = \frac{\omega^2}{\beta^2} \frac{1 - i \omega \mathcal{G}}{1 + \omega^2 \mathcal{G}^2} ,$$

where $\beta^2 = \frac{\mu}{\rho}, \mathcal{G} = \frac{\eta}{\mu}$. Solving the equation for the complex wave number

$$k_i = b - i a$$

formulas similar to the equations (3.24), (3.25) can be deduced

$$b = \frac{\omega}{\beta} \sqrt{\frac{1 + \sqrt{1 + \omega^2 \mathcal{G}^2}}{2(1 + \omega^2 \mathcal{G}^2)}} \tag{3.27}$$

$$a = \frac{\omega}{\beta} \sqrt{\frac{-1 + \sqrt{1 + \omega^2 \mathcal{G}^2}}{2(1 + \omega^2 \mathcal{G}^2)}} . \quad (3.28)$$

The wave's phase velocity $v_f = \frac{\omega}{b}$ is frequency dependent, so the transverse waves propagating in the Kelvin-Voigt medium show dispersion and their absorption coefficients is frequency dependent as well. In a low frequency border-line case $\omega \mathcal{G} \ll 1$. Then with series expansion the equations (3.27), (3.28) can be rewritten as

$$b = \frac{\omega}{\beta} \left(1 + \frac{1}{4} \omega^2 \mathcal{G}^2 \right) \approx \frac{\omega}{\beta}$$

$$a = \frac{\omega^2 \mathcal{G}}{2\beta} .$$

Thus in the first approximation the

$$v_f = \frac{\omega}{b} = \beta$$

phase velocity is frequency dependent, i.e. there is no dispersion, the absorption coefficient depends on the square of the frequency. The Kelvin-Voigt medium changes to Hooke body in low frequencies in point of view of wave propagation velocity, but it preserves the properties of the Newton body with respect to the absorption.

At high frequency $\omega \mathcal{G} \gg 1$. In this case the equations (3.27), (3.28) lead to the results reviewed at the Newton body

$$b = \sqrt{\frac{\rho \omega}{2\eta}} , \quad a = b .$$

The Kelvin-Voigt body gives back the Newton body in the high frequency border-line case. This can be expected from the structure of the model shown in Figure 2.1. The Kelvin-Voigt body is not suitable to describe weakly attenuating waves at high frequencies.

Longitudinal wave can be discussed by specifying the $rot \vec{s} = 0$, $rot \vec{v} = 0$ auxiliary conditions. As in this case the

$$rot \ rot \ \vec{s} = grad \ div \ \vec{s} - \Delta \vec{s} = 0$$

equation is satisfied, from the motion equation

$$\rho \frac{\partial^2 \bar{s}}{\partial t^2} = (\lambda + 2\mu)\Delta \bar{s} + (\zeta + 2\eta)\Delta \bar{v}.$$

Writing the time dependence in the form of $e^{i\omega t}$ the following equation can be formulated

$$\rho \frac{\partial^2 \bar{s}}{\partial t^2} = (\lambda + 2\mu)(I + i\omega \mathcal{G}_0)\Delta \bar{s}, \quad (3.29)$$

where $\mathcal{G}_0 = \frac{\zeta + 2\eta}{\lambda + 2\mu}$.

Based on the equation the

$$\lambda^* = \lambda(I + i\omega \mathcal{G}_0), \quad \mu^* = \mu(I + i\omega \mathcal{G}_0)$$

formulas can be introduced for the complex Lamé constants. With these the (3.29) can be rewritten as

$$\rho \frac{\partial^2 \bar{s}}{\partial t^2} = (\lambda^* + 2\mu^*)\Delta \bar{s}.$$

In search of the wave solution in the form of monochromatic plane wave

$$\bar{s} = \bar{s}^* e^{i(\omega t - k_i \bar{e} \bar{r})}$$

based on (3.29) the following complex dispersive equation can be derived

$$k_i^2 = \frac{\omega^2}{\alpha^2} \frac{I - i\omega \mathcal{G}_0}{I + \omega^2 \mathcal{G}_0^2}.$$

For the $k_i = b - ia$ wave number results similar to (3.27) and (3.28) can be obtained

$$b = \frac{\omega}{\alpha} \sqrt{\frac{I + \sqrt{I + \omega^2 \mathcal{G}_0^2}}{2(I + \omega^2 \mathcal{G}_0^2)}}, \quad a = \frac{\omega}{\alpha} \sqrt{\frac{-I + \sqrt{I + \omega^2 \mathcal{G}_0^2}}{2(I + \omega^2 \mathcal{G}_0^2)}},$$

from which the frequency dependent phase velocity

$$v_f = \frac{\omega}{b} = \alpha \sqrt{\frac{2(I + \omega^2 \mathcal{G}_0^2)}{I + \sqrt{I + \omega^2 \mathcal{G}_0^2}}}$$

and the frequency dependent penetration depth

$$d = \frac{\alpha}{\omega} \sqrt{\frac{2(I + \omega^2 \mathcal{G}_0^2)}{-I + \sqrt{I + \omega^2 \mathcal{G}_0^2}}}$$

can be deduced. These formulas have the form of

$$b = \frac{\omega}{\alpha}, \quad a = \frac{\omega^2 \mathcal{G}_0}{2\alpha}$$

$$v_f = \alpha, \quad d = \frac{2\alpha}{\omega^2 \mathcal{G}_0}$$

in the $\omega \mathcal{G}_0 \ll 1$ low frequency border-line case, i.e. the phase velocity has the value characteristic for the Hooke body, the absorption coefficient picks the value characteristic for the Newton body. The attenuation is weak, as $\omega \mathcal{G}_0 \ll 1$ is fulfilled trivially from the $a < b$ condition. The displacement function is

$$\bar{s} = \bar{s}_0 e^{-a\bar{r}} e^{i(\omega t - b\bar{r})}. \quad (3.30)$$

It should be understandable that the Kelvin-Voigt model is not appropriate for the description of weakly attenuating longitudinal waves in high frequency border-line case, because in that case

$$b = \sqrt{\frac{\rho \omega}{2(\zeta + 2\eta)}}, \quad a = b.$$

Note that the Kelvin-Voigt body can be applied with different \mathcal{G} parameters for the same rocks during description of rock mechanical and seismic phenomena. The characteristic time of creeping process in a rock has an order of magnitude of hours-days, a similar order of magnitude of \mathcal{G} retardation time belongs to this. However for description of weak attenuation of seismic waves the $\mathcal{G} = (10^{-3} - 10^{-5})(sec)$ value is suitable. This fact suggests that the Kelvin-Voigt model has an approximate validity, the \mathcal{G} parameter included in it is frequency dependent and it can be considered constant only in a narrow frequency range. However we can conclude that this model is suitable for description of weak attenuation of longitudinal and transverse waves. This is the reason that is widely used in seismics mostly for the description of wave propagation in rocks with high water and hydrocarbon content.

The constant Q model

The seismic experiences show that for most rocks the phase velocity is constant regardless to the frequency, but the absorption coefficient increases in direct proportion with the frequency

$$v_f = c \tag{3.31}$$

$$a = \frac{\omega}{2cQ}, \tag{3.32}$$

where Q is the frequency independent (constant) quality factor of rocks. This rock model is called the constant Q model.

In case of Hooke body (3.31) is satisfied, but there is no absorption. For the Kelvin-Voigt body (3.31) is satisfied at low frequency border-line case, the absorption coefficient can be determined by

$$a = \frac{\omega^2 \varrho}{2\beta},$$

i.e. compared to (3.32) $Q = \frac{I}{\omega \varrho}$, i.e. the quality factor is not constant. Similar results are obtained (at low frequency) for the Poynting-Thomson body. The Maxwell model can describe seismic waves in high frequency border-line case, but then

$$a = \frac{I}{\sqrt{2\tau\beta}},$$

i.e. based on (3.32) $Q = \frac{\omega\tau}{\sqrt{2}}$, the quality factor is proportional to the frequency. Similar results are obtained in high frequency border-line case by the Poynting-Thomson body.

It is understandable that the body following the constant Q model can be characterized by the complex Lamé constants

$$\mu^* = \mu(1 + i\varepsilon), \lambda^* = \lambda(1 + i\varepsilon') \tag{3.33}$$

if its material equation is assumed in the form similar to the Hooke body's formula (ε and ε' are frequency independent)

$$\sigma_{ik} = 2\mu^* \varepsilon_{ik} + \lambda^* \Theta \delta_{ik}.$$

The here presented dissipative rock physical parameters can be defined by the formulas

$$\varepsilon = \text{tg}(\delta), \varepsilon' = \text{tg}(\delta'),$$

where δ is the loss angle (the angle between the stress and the deformation in case of “pure” shear(for example at transverse waves)). δ' has similar interpretation in wave theory applications for the longitudinal waves.

Based on the stress tensor above the motion equation can be written as

$$\rho \frac{\partial^2 \bar{s}}{\partial t^2} = \mu^* \Delta \bar{s} + (\lambda^* + \mu^*) \text{grad div } \bar{s}. \quad (3.34)$$

For transverse waves $\text{div } \bar{s} = 0$ and so from the motion equation the

$$\rho \frac{\partial^2 \bar{s}}{\partial t^2} = \mu^* \Delta \bar{s}$$

equation can be derived. For the monochromatic waves written in the form of

$$\bar{s} = \bar{s}^* e^{i(\omega t - k_r \bar{e} r)}$$

using equation (3.33) the following dispersion equation can be deduced

$$k^2 = \frac{\omega^2}{\beta^2} \frac{1}{1 + i \varepsilon},$$

where $\beta^2 = \frac{\mu}{\rho}$. For the $k = b - i a$ complex wave number the

$$b = \frac{\omega}{\beta} \sqrt{\frac{1}{2(1 + \varepsilon^2)} (1 + \sqrt{1 + \varepsilon^2})} \quad (3.35)$$

$$a = \frac{\omega}{\beta} \sqrt{\frac{1}{2(1 + \varepsilon^2)} (-1 + \sqrt{1 + \varepsilon^2})} \quad (3.36)$$

equations can be written. It is easily understandable that we can speak about weak attenuation ($a < b$) only if $\varepsilon \ll 1$. Then with a simple series expansion from (3.35), (3.36) the following expressions can be derived

$$b = \frac{\omega}{\beta}$$

$$a = \frac{\omega \varepsilon}{2 \beta},$$

from which it can be seen after comparing to 3.32 that for transverse waves that the quality factor is really independent from the frequency

$$Q = \frac{1}{\varepsilon},$$

similar to the phase velocity $v_f = \frac{\omega}{b} = \beta$.

Stipulating the $\text{rot } \bar{s} = 0$ auxiliary condition for longitudinal waves the

$$\rho \frac{\partial^2 \bar{s}}{\partial t^2} = (\lambda^* + 2\mu^*) \Delta \bar{s}$$

equation can be deduced based on (3.34). In search for its monochromatic plane wave solution in the form of

$$\bar{s} = \bar{s}^* e^{i(\omega t - k_i \bar{e} \bar{r})}$$

the following dispersion equation can be obtained

$$k^2 = \frac{\omega^2}{\alpha^2} \frac{1}{1 + i\kappa},$$

where $\chi = \frac{\lambda \varepsilon' + 2\mu \varepsilon}{\lambda + 2\mu}$.

This equation changes into (3.35) with the substitution of $\alpha \rightarrow \beta, \chi \rightarrow \varepsilon$, therefore its solution can be written directly according to (3.35) and (3.36)

$$b = \frac{\omega}{\alpha} \sqrt{\frac{1}{2(1 + \chi^2)} \left(1 + \sqrt{1 + \chi^2} \right)} \quad (3.37)$$

$$a = \frac{\omega}{\alpha} \sqrt{\frac{1}{2(1 + \chi^2)} \left(-1 + \sqrt{1 + \chi^2} \right)}. \quad (3.38)$$

Weak attenuation happens only if $\chi^2 \ll 1$ (i.e. $\varepsilon \ll 1, \varepsilon' \ll 1$), therefore based on (3.37), (3.38)

$$b = \frac{\omega}{\alpha}, \quad a = \frac{\omega \chi}{2\alpha}.$$

Based on the comparison to (3.32) the quality factor for longitudinal waves can be obtained in the form

$$Q = \frac{1}{\chi} = \frac{\lambda + 2\mu}{\lambda \varepsilon' + 2\mu \varepsilon}.$$

The constant Q model gained widespread application in the field of seismics and acoustics.

References

Asszonyi Cs., Richter R. 1975: *Bevezetés a kőzetmechanika reológiai elméletébe*. Nehézipari Minisztérium Továbbképző Központja, Budapest.

4. Elastic wave propagation

The pressure dependence of elastic properties of acoustic waves is an extensively explored rock physical problem because pressure strongly influences the mechanical and transport properties of rocks, such as acoustic velocity, porosity, permeability and resistivity. By using the discussed elastic medium models in the previous sections petrophysical models can be developed which describe the pressure dependence of elastic properties of rocks (primarily the velocity-pressure and quality factor-pressure relationships). By the knowledge of the characteristics of elastic waves - if this dependence can be reversed - stress state of rocks can be determined indirectly based on seismic/acoustic measurements in laboratory. To relate changes in seismic attributes to reservoir conditions, a thorough understanding of pressure effects on rock properties is essential.

4.1. Describing the pressure dependence of longitudinal wave velocity

The velocity of acoustic waves propagating in different rocks under various confining pressure conditions (Wyllie *et al.* 1958, Stacey 1976, Prasad and Manghnani 1997, King 2009) and also under different pore pressures (Nur and Simmons 1969, Yu *et al.* 1993, Darot and Reuschlé 2000, He and Schmitt 2006) were investigated for several decades by many researchers. According to general observations, larger propagation velocities are measured on water-saturated samples than on dry or gas-saturated ones (Toksöz *et al.* 1976) and the P wave velocity is larger in coarse grained, sedimentary rocks than that of in fine grained samples (Prasad and Meissner 1992). The phenomenon that the wave velocity increases with pressure is well-known and has been explained on various rock mechanical studies (Wyllie *et al.* 1956, Birch 1960). One of the most frequently used mechanisms for explaining the phenomenon is based on the closure of microcracks in rocks under the change of pressure (Holt *et al.* 1997; Best 1997; Hassan and Vega 2009; Sengun *et al.* 2011). Singh *et al.* (2006) created an empirical model for the pressure dependent wave velocity after observing measured P and S wave velocities on several sandstone samples. Prasad (2002) studied the same relationship for gas-saturated and pressurized zones from the ratio of propagation velocities of P and S waves.

According to petrophysical models and experimental results, we can infer to the size of emerging tensions in rocks, and even probably to its dependence of direction using measured longitudinal and transversal wave velocity data. Several petrophysical models can be found in the literature, e.g., Biot model (Biot 1956a, Biot 1956b), Gassmann model (Gassmann 1951), Contact radius model (Duffy and Mindlin 1957), Friction model (Winkler and Nur

1982, Stewart *et al.* 1983), etc. These models provide proper approach for the description of the phenomena depending on the type of rock. The Biot model for example describes wave propagation in a two phase system, a porous elastic frame and a viscous, incompressible pore fluid. The propagation and attenuation of the wave is ascribed to relative motion between the frame and its pore fluid.

In the lecture notes we present a new approach for the quantitative description of the pressure dependence of phase velocity of acoustic waves. Our considerations are based on the mechanism that microcracks are closing with increasing pressure.

4.1.1. The pressure dependent acoustic velocity model

Modeling plays an important role in the cognition of natural science. In the explanation of a phenomena we consider the most important and most essential properties and neglect all the other (in other aspects may be important) characteristics. Hence, we set up a model in which we simplify the studied structure and henceforth we talk about the properties of the model. This approach was followed at the development of the pressure dependent velocity model.

The response of rock to stress depends on its microstructure and constituent minerals, which is manifested in pressure dependence of velocity of elastic waves. Several qualitative ideas exist describing the pressure dependence of seismic velocity. Such as that pore volume reduces with increasing pressure, thus increasing velocity can be measured (Birch 1960). Following Brace and Walsh (1964) we assume that the main factor determining the stress dependence of the wave propagation velocity is the closure of the microcracks. For this reason, we introduce parameter N as the number of open microcracks. Accepting this qualitative idea a rock physical model – which is valid only in the reversible (elastic) range - was developed using the following formulation. (In our considerations we focus on uniaxial stress state and longitudinal acoustic waves.)

If we create a stress increase $d\sigma$ in the rock, we find that dN (the change of the number of open microcracks) is directly proportional to the applied stress increase $d\sigma$. At the same time dN is directly proportional to N . We can unify both assumptions in the following differential equation as

$$dN = -\lambda N d\sigma, \quad (1)$$

where λ is a new material dependent petrophysical constant. In Eq. (1) the negative sign represents that at increasing stress - with closing microcracks - the number of the open microcracks decreases. The solution of Eq. (1) is

$$N = N_0 \exp(-\lambda\sigma), \quad (2)$$

where N_0 is the number of the open microcracks at stress-free state ($\sigma = 0$). Another assumption is a linear relationship between the propagation velocity change dv - due to pressure increment $d\sigma$ - and dN

$$dv = -\alpha dN, \quad (3)$$

where α is another proportionality factor (material quality dependent constant). The negative sign represents that the velocity is increasing with decreasing number of cracks. Combining Eq. (3) with Eq. (1) and Eq. (2) we obtain

$$dv = \alpha\lambda N_0 \exp(-\lambda\sigma) d\sigma. \quad (4)$$

Solving the upper differential equation we have

$$v = K - \alpha N_0 \exp(-\lambda\sigma). \quad (5)$$

where K is an integration constant. At stress-free state ($\sigma = 0$) the propagation velocity v_0 can be measured and computed from Eq. (5) as $v_0 = K - \alpha N_0$. Hence, we obtain the integration constant: $K = v_0 + \alpha N_0$. With this result and the introduction of $\Delta v = \alpha N_0$, Eq. (5) can be rewritten in the following form

$$v = v_0 + \Delta v (1 - \exp(-\lambda\sigma)). \quad (6)$$

Eq. (6) provides a theoretical connection between the propagation velocity and rock pressure. The model equation shows that the propagation velocity - as a function of stress - starts from v_0 and increases up to the $v_{max} = v_0 + \Delta v$ value according to the function of $1 - \exp(-\lambda\sigma)$. Thus, the value $\Delta v = v_{max} - v_0$ specifies a velocity range in which the propagation velocity can vary from stress-free state up to the state characterized by high rock pressure.

The velocity reaches its limit v_{max} at high stress values. Certainly it is only valid in the framework of the model assumptions (reversible range), because in the range of high stresses new microcracks can arise in the rock. (This phenomenon is outside of our present considerations. In order not to exceed reversible range and to avoid creating new cracks, samples were loaded during our measurements only up to one third of the critical uniaxial strength.)

Since λ is a new petrophysical parameter (material characteristic) it is necessary to give its physical meaning. Introducing the notation $u = v_{max} - v$, wherewith Eq. (6) can be written also in the form

$$u = \Delta v \exp(-\lambda\sigma). \quad (7)$$

It can be seen that at the characteristic stress σ^* (when $\lambda\sigma^*=1$) the quantity $v_{max} - v$ decreases from its Δv „initial” value to $\Delta v/e$. The λ petrophysical characteristic (material constant) is the reciprocal value of σ^* . On the other hand, we can also give another meaning of parameter λ .

The experiences show that rocks show different velocity response to the same change in the rock pressure or in other words the velocity shows different sensitivity to pressure. It is interesting to see, what amount of (relative) velocity change can be measured as a consequence of a certain (for example unit) change in the stress. For similar purpose the sensitivity functions are extensively used in the seismic (Dobróka 1987), the geoelectric (Gyulai 1989), electromagnetic (Szalai and Szarka 2008) and well-logging (Dobróka and Szabó 2011) literature. So, we introduce the (logarithmic) stress sensitivity of the $u = v_{max} - v$ velocity as

$$S(\sigma) = -\frac{1}{u} \frac{du}{d\sigma} = -\frac{d \ln(u)}{d\sigma}. \quad (8)$$

Using Eq. (7) it can be seen that

$$\lambda = -\frac{d \ln(u)}{d\sigma} = S, \quad (9)$$

which shows that the λ petrophysical characteristic is the logarithmic stress sensitivity of the $u = v_{max} - v$ velocity. It can be seen that in our petrophysical model the logarithmic stress sensitivity is independent of the stress.

4.1.2. Experimental setting, technique and samples

The pulse transmission technique (Toksöz *et al.* 1979) was used for P wave velocity measurements. The experimental set-up (Fig. 1) was compiled at the Department of Geophysics (University of Miskolc). Rock samples subjected to uniaxial stress were analyzed with an electromechanical pressing device and wave velocities - as a function of pressure - were measured at adjoining pressures.

An important question is that how reproducible the measurements are. Hence we made time-lapse measurements in case of several samples. One typical test result is presented in Fig. 2.

It was shown that the second measurement provided the same result with very good approximation. Thus the phenomenon is highly reproducible and the elastic range was not exceeded (new microcracks were not formed under pressure).

The specimens used in our studies originated from oil-drilling wells. We performed wave velocity measurements on several different air-dried sandstone samples. Three typical

test results (sample S1, S2 and S3) are presented in this lecture notes. Table 1 contains the description and depths of our studied samples.

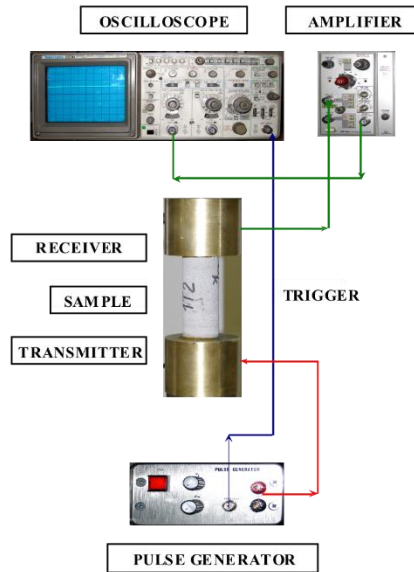


Figure 1.: Measurement layout for wave velocity measurements

Table 1.: Characteristics of our experimental samples

Sample	Description	Depth [m]
S1	Fine-, medium-grained sandstone	2800
S2	Fine-grained sandstone	3500
S3	Tuffy sandstone	2800

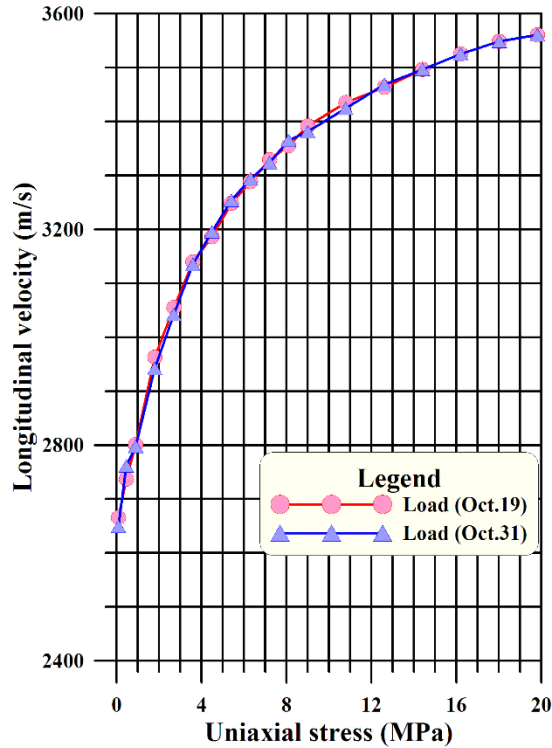


Figure 2.: Result of repeated measurements for studying reproducibility

4.1.3. Case studies

The parameters appearing in the model equation (Eq. (6)) can be determined by processing measurement data based on the method of geophysical inversion (Dobróka *et al.* 1991, Dobróka and Szabó 2005). In order to prove the validity and practical applicability of the velocity model introduced in Section 2, we present the results of the applied linearized inversion method for each sample (Table 2). The inverse problem is overdetermined, so the Least Squares method (Menke 1984) can be effectively used for solving it.

Table 2.: Model parameters estimated by linearized inversion

Sample	v_0 [m/s]	Δv [m/s]	λ [1/MPa]
S1	2571,1	827,8	0,1471
S2	2561,6	753,5	0,2157
S3	3280,9	476,6	0,2774

With the estimated parameters the velocities can be calculated at any pressure by substituting them into Eq. (6). The results are shown in Figs. 3-5. The continuous line shows the calculated velocity-pressure function while asterisk symbols represent the measured data.

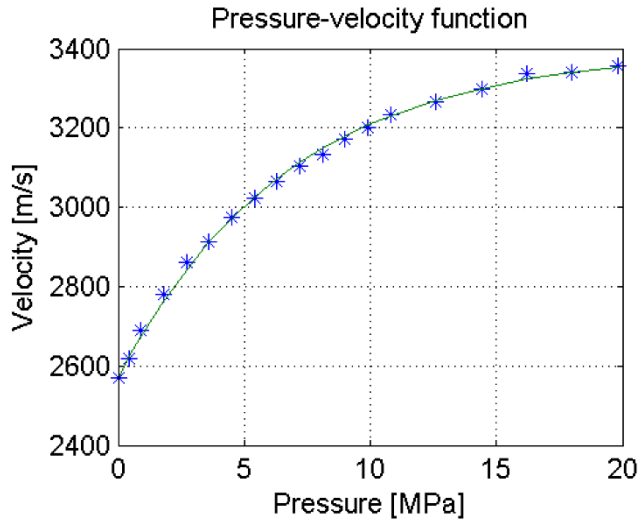


Figure 3.: Longitudinal wave velocity-pressure function on sample S1 (continuous line – calculated data produced by inversion, asterisks – measured data)

Figs. 3-5 show that the calculated curves are in good accordance with the measured data which proves that the petrophysical model suggested in Eq. (6) applies well in practice. It can be seen that in the lower pressure regime, the increase in velocity with increasing pressure is very steep and nonlinear. This is due to the closure of microcracks, which dramatically affects the elastic properties of rock and thereby the velocities. In the higher pressure regime, the increase in velocity (with increasing pressure) is moderate as fewer numbers of cracks closed. The model was also applied on several sandstone samples (fine-, medium-, coarse-grained, pebbly, tuffey etc.) during the research and similar results were obtained.

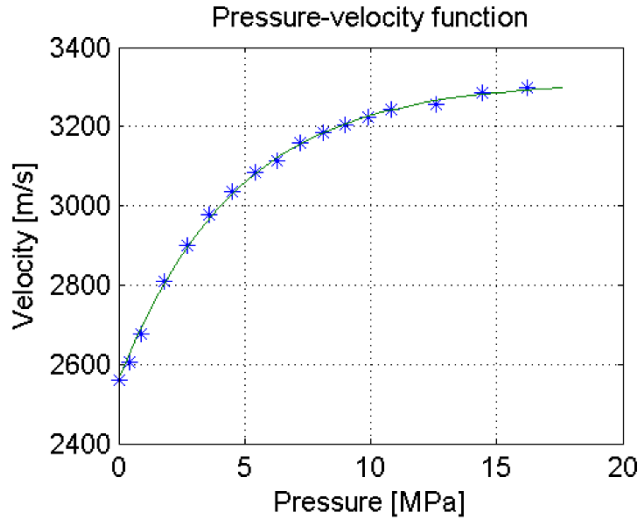


Figure 4.: Longitudinal wave velocity-pressure function on sample S2 (continuous line – calculated data produced by inversion, asterisks – measured data)

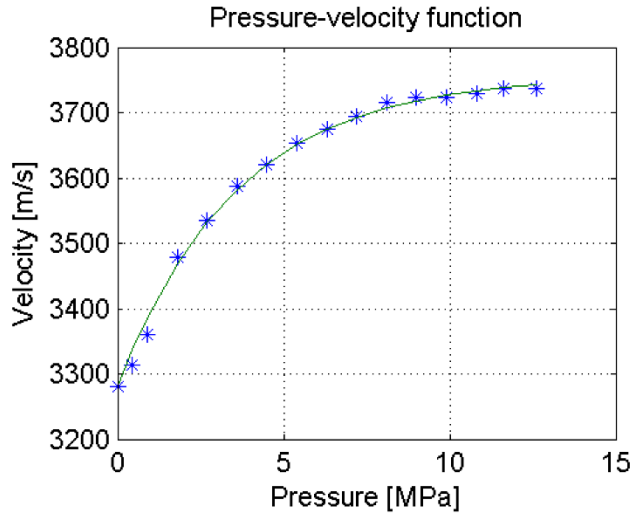


Figure 5.: Longitudinal wave velocity-pressure function on sample S3 (continuous line – calculated data produced by inversion, asterisks – measured data)

As it was mentioned the samples were loaded during our measurements only up to one third of the critical uniaxial strength. It was found that λ is connected with uniaxial strength:

the higher the uniaxial strength of a sample, the smaller the estimated λ is. It was also observed that the parameter v_0 is sensitive to rock quality, as it can be seen in Fig. 6. Since sample S1 was a fine-, medium-grained and S2 was fine-grained sandstone, the curves belong to these samples are almost the same. But the curve of the tuffy sandstone sample (S3) is located in different velocity range, because it starts from a different initial velocity (v_0). Finding connection between the other parameters and rock quality requires further investigations.

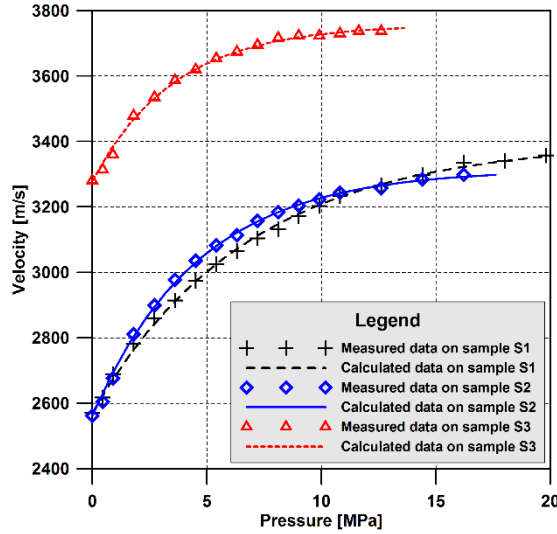


Figure 6.: Longitudinal wave velocities as a function of pressure for the studied samples (curves – calculated data produced by inversion, symbols – measured data)

For the characterization of the accuracy of estimations, we calculated the measure of fitting according to the data misfit ($D[\%]$) formula

$$D = \sqrt{\frac{1}{N} \sum_{k=1}^N \left(\frac{d_k^{(m)} - d_k^{(c)}}{d_k^{(c)}} \right)^2} \cdot 100 [\%], \quad (10)$$

where $d_k^{(m)}$ is the measured velocity at the k -th pressure and $d_k^{(c)}$ is the k -th calculated velocity data, which can be computed according to Eq. (6). Table 3 contains the value of data misfits for each sample in the last iteration step.

Table 3.: Values of the calculated measure of fitting in data space

Sample	D [%]
S1	0,30
S2	0,29
S3	0,34

References

- Best, A.I. (1997), The effect of pressure on ultrasonic velocity and attenuation in near-surface sedimentary rocks, *Geoph. Prosp.* **45**, 345-364, DOI: 10.1046/j.1365-2478.1997.00344.
- Biot, M.A. (1956a), Theory of propagation of elastic waves in fluid saturated porous solids, I: Low frequency range, *J. Acoust. Sot. Am.* **28**, 168-178, DOI: 10.1121/1.1908239.
- Biot, M.A. (1956b), Theory of propagation of elastic waves in fluid saturated porous solids, II: High frequency range, *J. Acoust. Sot. Am.* **28**, 179-191, DOI: 10.1121/1.1908241.
- Birch, F. (1960), The velocity of compression waves in rocks to 10 kilobars, Part 1, *J. Geophys. Res.* **65**, 1083-1102, DOI: 10.1029/JZ065i004p01083.
- Brace, W.F., and J.B. Walsh (1964), A fracture criterion for brittle anisotropic rock, *J. Geophys. Res.* **69**, 3449-3456, DOI: 10.1029/JZ069i016p03449.
- Darot, M., and T. Reuschlé (2000), Acoustic wave velocity and permeability evolution during pressure cycles on a thermally cracked granite, *Int. J. Rock. Mech. Min. Sci.* **37**, 1019-1026, DOI: 10.1016/S1365-1609(00)00034-4.
- Dobróka, M. (1987), Love seam-waves in a horizontally inhomogeneous three-layered medium. *Geoph. Prosp.* **35**, 512-516, DOI: 10.1111/j.1365-2478.1987.tb00832.
- Dobróka, M., Á. Gyulai, T. Ormos, J. Csókás, L. Dresen (1991), Joint inversion of seismic and geoelectric data recorded in an underground coal-mine, *Geoph. Prosp.* **39**, 643-665, DOI: 10.1111/j.1365-2478.1991.tb00334.
- Dobróka, M., and N.P. Szabó (2005), Combined global/linear inversion of well-logging data in layer-wise homogeneous and inhomogeneous media. *Acta Geod. Geoph. Hung.* **40**(2), 203-214.
- Dobróka, M., and N. Szabó (2011), Interval inversion of well-logging data for objective determination of textural parameters, *Acta Geophysica.* **59**(5), 907-934, DOI: 10.2478/s11600-011-0027-z.
- Duffy, J., and R.D. Mindlin (1957,) Stress-strain relations and vibrations of a granular medium, *J. Appl. Mech.* **24**, 585-593.

- Gassmann, F. (1951), *Über die Elastizität poröser Medien*, Viertel Naturforsch Ges Zürich.
- Gyulai, Á. (1989), Parameter sensitivity of underground DC measurements, *Geophysical transactions*. **35**(3), 209-225.
- Hassan, A., and S. Vega (2009), A study of seismic velocities and differential pressure dependence in a Middle East carbonate reservoir. **In: Proc. 79th SEG International Exposition and Annual Meeting, 25-30 October 2009, Houston, USA**, DOI: 10.1190/1.3255765.
- He, T., and D.R. Schmitt (2006), Velocity measurements of conglomerates and pressure sensitivity analysis of AVA response. **In: Proc. 76th SEG International Exposition and Annual Meeting, 1-6 October 2006, New Orleans, USA**, DOI: 10.1190/1.2369894.
- Holt, R.M., A.K. Furre, P. Horsrud (1997), Stress dependent wave velocities in sedimentary rock cores: why and why not?, *Int. J. Rock. Mech. Min. Sci.* **34**, 3-4, DOI: 10.1016/S1365-1609(97)00059-2.
- King, M.S. (2009), Recent developments in seismic rock physics, *Int. J. Rock. Mech. Min. Sci.* **46**, 1341-1348, DOI: 10.1016/j.ijrmms.2009.04.008.
- Menke, W. (1984), *Geophysical data analysis – Discrete inverse theory*, Academic Press, London.
- Nur, A., and G. Simmons (1969), The effect of saturation on velocity in low porosity rocks, *Earth Planet Sci. Lett.* **7**, 183-193, DOI: 10.1016/0012-821X(69)90035-1.
- Prasad, M., and R. Meissner (1992), Attenuation mechanism in sands: Laboratory versus theoretical (Biot) data, *Geophysics*. **57**(5), 719-710, DOI: 10.1190/1.1443284.
- Prasad, M., and M.H. Manghnani (1997), Effects of pore and differential pressure on compressional wave velocity and quality factor in Berea and Michigan sandstones, *Geophysics*. **62**(4), 1163-1176, DOI: 10.1190/1.1444217.
- Prasad, M. (2002), Acoustic measurements in unconsolidated sands at low effective pressure and overpressure detection, *Geophysics*. **67**(2), 405-412, DOI: 10.1190/1.1468600.
- Sengun, N., R. Altindag, S. Demirdag, H. Yavuz (2011), P-wave velocity and Schmidt rebound hardness value of rocks under uniaxial compressional loading, *Int. J. Rock. Mech. Min. Sci.* **48**, 693-696, DOI: 10.1016/j.ijrmms.2011.02.007.
- Singh, R., C. Rai, C. Sondergeld (2006), Pressure dependence of elastic wave velocities in sandstones. **In: Proc. 76th SEG International Exposition and Annual Meeting, 1-6 October 2006, New Orleans, USA**.

- Stacey, T.R. (1976), Seismic assessment of rock masses. **In:** *Proc. Symp on Exploration for Rock Engineering, 1-5 November 1976, Johannesburg, South Africa.*
- Stewart, R.D., M.N. Toksöz, A. Timur (1983), Strain dependant attenuation: observations and a proposed mechanism, *J. Geophys. Res.* **88**, 546-554, DOI: 10.1029/JB088iB01p00546.
- Szalai, S., and L. Szarka (2008), Parameter sensitivity maps of surface geoelectric arrays, I. Linear arrays, *Acta Geod. Geoph. Hung.* **43**, 419-437, DOI: 10.1556/ageod.43.2008.4.4.
- Toksöz, M.N., C.H. Cheng, A. Timur (1976), Velocities of seismic waves in porous rocks, *Geophysics.* **41**(4), 645-621, DOI: 10.1190/1.1440639.
- Toksöz, M.N., D.H. Johnston, A. Timur (1979), Attenuation of seismic waves in dry and saturated rocks, I. Laboratory measurements, *Geophysics.* **44**(4), 681-690, DOI: 10.1190/1.1440969.
- Winkler, K.W., and A. Nur (1982), Seismic attenuation: effects of pore fluid and frictional sliding, *Geophysics.* **47**, 1-15.
- Wyllie, M.R.J., A.R. Gregory, G.H.F. Gardner (1956), Elastic wave velocities in heterogeneous and porous media, *Geophysics.* **21**(1), 41–70, DOI: 10.1190/1.1438217.
- Wyllie, M.R.J., A.R. Gregory, G.H.F. Gardner (1958), An experimental investigation of factors affecting elastic wave velocities in porous media, *Geophysics.* **23**(3), 459-493, DOI: 10.1190/1.1438493.
- Yu, G., K. Vozoff, D.W. Durney (1993), The influence of confining pressure and water saturation on dynamic elastic properties of some Permian coals, *Geophysics.* **58**(1), 30-38, DOI: 10.1190/1.1443349.

4.2. Describing the pressure dependence of quality factor

In recent years, the attenuation of seismic waves has found increased interest as an important parameter for rock characterization. Attenuation as a function of depth has fundamental interest in groundwater, engineering, and environmental studies as well as in oil exploration and earthquake seismology. As is well-known, compared to the phase velocity, the absorption coefficient is much more sensitive for the pressure change. So the discussion of the pressure dependence of the absorption coefficient or that of the seismic Q can be interesting also in the exploration of near surface structures.

Theories of seismic wave attenuation in rocks (Mavko *et al.* 1979; Bourbié *et al.* 1987) usually include the nonlinear friction model, the Biot model, viscoelastic models and elastic scattering. According to the frictional model the attenuation is caused by the anelasticity of the rock matrix and frictional dissipation due to relative motions at grain boundaries (White

1966) and across crack surfaces (Walsh 1966). The Biot model (Biot 1956a,b) explains the dissipation in a fully saturated rock by the relative motion between the solid components and pore-fluid. The viscoelastic model (Bland 1960) contains numerous physical mechanisms, viz. "squirt" or "squish" flow, mechanical defects of rocks (such as anelasticity of cracks), grain-scale local flow, and viscous relaxation. Attenuation predicted by the elastic scattering mechanism is a geometric effect caused by scattering off small pores (Kuster and Toksöz 1974) or selective reflection of thin beds (O'Doherty and Anstey 1971).

The propagation characteristics of seismic wave carry information of important mechanical properties of rocks, therefore the determination of attenuation and velocity of acoustic wave is a frequent task in laboratory. Laboratory measurements of attenuation have been made at seismic frequencies (Spencer 1981; Dunn 1987; Paffenholz and Burkhardt 1989), sonic frequencies (Murphy 1982; Lucet *et al.* 1991) and more commonly at ultrasonic frequencies (Toksöz *et al.* 1979; Winkler 1985; Khazanehdari and McCann 2005; Han *et al.* 2011). Measurements done under different pressure conditions are useful for understanding the mechanisms of attenuation. The pressure dependence of velocity and attenuation of P and S waves were measured on dry, water-, brine-, methane-saturated as well as frozen samples by Toksöz *et al.* (1979). It was found that the attenuation was higher in case of fresh water- and brine-saturated samples than in methane-saturated or dry samples. Some significant characteristics of the attenuation behaviour of sedimentary rocks were also shown in the example of Berea sandstone by Toksöz *et al.* (1979). The experimental results showed that attenuation decreased with increasing pressure for P waves. This dependence is nonlinear and distinct changes are present at low pressures. In the higher pressure range, the change of grain contacts and porosity is smaller. As the reason of this phenomenon the closure of microcracks under varying pressure was noted by various authors (Johnston *et al.* 1979, Yu *et al.* 1993, Best 1997). Bastiaens (2005) studied the EDZ (Excavation Disturbed or Damaged Zone) around the gallery by observing macro-fractures and pore pressure distribution. It was shown that the orientation of all fractures indicating a consistent fracture pattern along the gallery and industrial excavation techniques can limit the EDZ. Prasad and Meissner (1992) have studied the influence of grain size, grain shape, and differential pressure on compressional and shear wave velocity and attenuation at frequencies of 100 kHz. Their measurements show that coarser grains make the velocity and attenuation of compressional waves increase and angularity of grains causes a decrease in velocity and attenuation.

To evaluate laboratory measurements reliably, a quantitative model of the mechanism of pressure dependence of the dispersion characteristics is required. In this lecture notes a

petrophysical model is introduced which explains the mechanism of pressure dependence of attenuation of seismic waves. The petrophysical model is tested on laboratory measurement data published earlier by Toksöz *et al.* (1979), Lucet and Zinszner (1992), Yu *et al.* (1993), Meglis *et al.* (1996) as well as Prasad and Manghnani (1997).

4.2.1. The pressure dependent seismic q model

Modelling plays an important role in the cognition of natural science. The phenomena of the material world usually cannot be described in their entirety because of their complexity. Toksöz and Johnston (1981) distinguish two lines of the mathematical and physical descriptions for attenuation mechanism. The first type of theories and models uses physical and mathematical descriptions of possible attenuation mechanisms. These mechanisms are related to the microscopic properties of the rock and their behaviour during elastic wave propagation. The second method is to explain the nature of attenuation in terms of generalized equation of linear elasticity (Hooke's law) or by modified equations allowing certain nonlinearity. These phenomenological models consider the most important and essential properties neglecting all the other (in other aspects may be important) characteristics. Rocks are in general heterogeneous and often replaced by an effective or equivalent homogeneous material within a representative elemental volume if the dimensions of the constituents (e.g. grains, pores, cracks) are small compared with the shortest seismic wavelength. Based on the latter, we set up a model in which we simplify the studied structure and henceforth we talk about the properties of the model. A material with small-scale variations in properties (permeated with cracks) acts mechanically as homogeneous medium if the excitation wavelengths are large compared with the scale of the variations in the structure. At the development of our rock physical model we assumed the macroscopic homogeneity of rocks.

The attenuation in a rock medium is defined by the well-known formula given by Knopoff (1965)

$$a = \frac{\pi f}{Qv}, \quad (1)$$

where a is the absorption coefficient, f is the frequency, Q is the quality factor and v is the propagation velocity of acoustic wave. The most common measure of seismic-wave attenuation is the dimensionless quality factor Q or its inverse Q^{-1} (dissipation factor). The quality factor as an intrinsic rock property represents the ratio of stored to dissipated energy. It is a general observation that the presence of microcracks, fractures and other defects in the solid

rock material results in significant pressure dependence of attenuation (i.e. it decreases with increasing pressure), and velocity (i.e. it increases with increasing pressure) as a result of fracture closing and improved contacts (Klíma *et al.* 1964, Gordon and Davis 1968, Johnston *et al.* 1979). Walsh (1966) approximated the cracks within the rocks by ellipsoids in plane strain with a small aspect ratio. Based on the frictional model the pressure-attenuation relationship can be characterized by the exponential decrease of attenuation with increasing pressure (Schön 1996). The character of the exponential function depends on the aspect ratio and the effective static frame bulk modulus. The attenuation coefficient vs. pressure dependence of sands at low pressure can also be described by a simple power law (Schön 1996) $a = a_0(p/p_0)^n$, where p is the pressure, p_0 the reference pressure (e.g., 1 kPa), a_0 the attenuation coefficient at this pressure, and n an exponent. It must be noted that in this case the phenomenon of pressure dependence can be explained based on the change of pore volume under pressure instead of microcracks. The data from Hunter *et al.* (1961) lead to a value of $n = 1/6$. Hamilton (1976) gives values between $1/6$ and $1/2$ for sediments saturated with water.

To reasonably interpret laboratory measurements, a quantitative model - which provides the physical explanation - of the mechanism of pressure dependence is required, which includes as few parameters as possible. Several qualitative ideas exist to explain pressure dependence. One such idea is that with increasing pressure the pore volume reduces, thus increasing quality factor and velocity can be measured (Birch 1960). Brace and Walsh (1964) explained the phenomenon of pressure dependence by the closure of microcracks. Accepting this qualitative idea we can create a simple petrophysical model based on the following formulation. We studied the effect of microcracks on the quality factor by means of quantitative considerations without so much as the detailed analysis of the structural mechanisms. In our considerations we restrict the problem to uniaxial stress state and longitudinal acoustic waves and it is also assumed, that the Q-factor is independent of the frequency (the so-called constant Q-model - which connected to the frictional attenuation - is used with allowing the changes due to the stress variations).

If we create stress increase ($d\sigma$), in the rock, we assume that dN (the change of the number of open microcracks) is directly proportional to the stress increment, $d\sigma$. At the same time, dN is directly proportional to N , which is the total number of open microcracks (per unit volume). We can unify both assumptions in the following differential equation as

$$dN = -\lambda N d\sigma, \quad (2)$$

where λ is a proportionality factor (constant depends on material quality). In Eq.(2) the negative sign represents that at increasing stress - with closing microcracks - the number of the open microcracks decreases. The solution of the upper equation is well-known

$$N = N_0 \exp(-\lambda\sigma), \quad (3)$$

where N_0 is the number of the open microcracks at stress-free state ($\sigma = 0$). It can be seen that at the characteristic stress σ^* (when $\lambda\sigma^*=1$) the quantity N - which is the crack density after Meglis *et al.* (1996) in unit volume - decreases from its „initial” value N_0 to N_0/e . Hence the petrophysical parameter λ is the reciprocal value of the characteristic stress σ^* , which provides the physical meaning of parameter λ . The only problem with this interpretation of λ is that the crack density in Eq.(3) is not directly measurable. Thus, it is required to be connected to measurable quantities, e.g. seismic Q . On the other hand it is obvious that the increase in dN leads to a decrease in the change of quality factor (dQ), hence we assume a linear relationship between these infinitesimal changes

$$dQ = -\alpha dN, \quad (4)$$

where α is another proportionality factor (material quality dependent constant). The negative sign represents that the quality factor is increasing with decreasing number of open microcracks. Combining the previous assumptions we obtain

$$dQ = \alpha\lambda N_0 \exp(-\lambda\sigma) d\sigma. \quad (5)$$

After integrating Eq.(5) we have

$$Q = K - \alpha N_0 \exp(-\lambda\sigma). \quad (6)$$

At stress-free state ($\sigma=0$) the quality factor can be measured in the rock sample. Its value is denoted by Q_0 and can be computed from Eq.(6) as $Q_0 = K - \alpha N_0$. Thus we obtain the integration constant: $K = Q_0 + \alpha N_0$. With this result and the introduction of $\Delta Q_0 = \alpha N_0$, Eq.(6) can be rewritten in the following form

$$Q = Q_0 + \Delta Q_0 (1 - \exp(-\lambda\sigma)). \quad (7)$$

It is well-known that there can be several reasons to absorption. Using Eq. (7) - which provides a theoretical connection between the quality factor and rock pressure - we describe the attenuation caused by only the change in the number of microcracks under varying pressure. The quality factor as a function of stress starts from Q_0 and increases up to the value $Q_{max}=Q_0+\Delta Q_0$ according to the function $1-\exp(-\lambda\sigma)$. The value $\Delta Q_0 = Q_{max}-Q_0$ is the range in which the

quality factor can increase from stress-free state up to the state characterized by high rock pressure. From the notation $\Delta Q_0 = \alpha N_0$ it follows that in case of samples originated from the same rock type (same geological unit), when α can be considered (nearly) as constant, ΔQ_0 is proportional to the number of open microcracks (per unit volume) N_0 . Namely if ΔQ_0 is small in a rock sample, the related number of open microcracks is low.

The quality factor reaches its upper limit Q_{max} at high stress values. Certainly it is only valid in the framework of the model assumptions, because in the range of (very) high stresses new microcracks can arise in the rock. Therefore the developed model is valid only in the so-called reversible range. (Description of non-reversible range is outside of our present considerations.)

Since λ is a new petrophysical parameter (material characteristic) it is necessary to give its physical meaning. As it was mentioned before, the petrophysical characteristic λ (material constant) is the reciprocal value of the characteristic stress σ^* . However another meaning of parameter λ can be given. Introducing the quantity $\Delta Q = Q_{max} - Q$ (the available range in which the quality factor can increase from a certain pressure up to the state characterized by high rock pressure), wherewith Eq. (7) can be written also in the form

$$\Delta Q = \Delta Q_0 \exp(-\lambda \sigma). \quad (8)$$

Laboratory experiments show that rocks have different quality factor response to the same change in the rock pressure or in other words the quality factor exhibits different sensitivity to pressure change. For similar purpose the sensitivity functions are extensively used in the seismic, well-logging, electromagnetic and geoelectric literature (Gyulai 1989). So, we introduce the (logarithmic) stress sensitivity of the quality factor change $\Delta Q = Q_{max} - Q$ as

$$S(\sigma) = -\frac{1}{\Delta Q} \frac{d(\Delta Q)}{d\sigma} = -\frac{d \ln(\Delta Q)}{d\sigma}. \quad (9)$$

Using Eq. (8) it can be seen that

$$\lambda = -\frac{d \ln(\Delta Q)}{d\sigma} = S, \quad (10)$$

which shows that the petrophysical characteristic λ is the logarithmic stress sensitivity of the quality factor, $\Delta Q = Q_{max} - Q$. It can be seen that in our petrophysical model the logarithmic stress sensitivity is independent of stress. It is noted that after the determination of λ it can be considered as the reciprocal value of the characteristic stress σ^* at which the crack density decreases from its „initial” value N_0 to N_0/e .

4.2.2. The pressure dependent propagation velocity

The velocity of elastic waves in rocks are influenced primarily by the elastic properties of the rock forming minerals, relative volumes of minerals, consolidation and cementation of the rock matrix, porosity, pore shape and content, pressure and temperature. It is well-known that the velocity of acoustic wave propagating in rocks is nonlinearly connected with the effective pressure (Yu *et al.* 1993, Best 1997). For an analytical description of the nonlinear velocity vs. pressure relationship, exponential functions are most commonly used (Wepfer and Christensen 1991; Wang *et al.* 2005; Singh *et al.* 2006). Several empirical models exist to describe the pressure dependence of longitudinal acoustic wave velocity, but these models usually provide the determination of the parameters of a suitably chosen formula based on mathematical regression method remaining the physical meaning unexplained (Wepfer and Christensen 1991, Ji *et al.* 2007). A phenomenological theory for fractured rocks after Schön (1996) describes the effect of all defects (fractures, defects at grain boundaries, intragranular defects, etc.) by one parameter. Wang *et al.* (1971) showed the application of this simple model describing the velocity vs. depth function on terrestrial and lunar rock specimens.

At the development of our velocity model - similarly to the quality factor model - we assume linear relationship between the propagation velocity change dv and the number of closing microcracks dN (due to pressure increment $d\sigma$)

$$dv = -\beta dN . \tag{11}$$

where β is the proportionality factor (another material quality dependent constant introduced by Dobróka and Somogyi Molnár (2012). The negative sign represents that the velocity is increasing with decreasing number of cracks. Our theory is based on that the same change in the number of microcracks refers to the pressure dependence of quality factor and also that of velocity. (Meglis *et al.* (1996) experimentally proved that the crack density parameter derived from measurement of pressure dependence of quality factor and velocity is the same for both quantities.) Combining this assumption with Eq.(2) and Eq.(3) we obtain

$$dv = \beta \lambda N_0 \exp(-\lambda \sigma) d\sigma . \tag{12}$$

After solving Eq.(12) we have

$$v = v_0 + \beta N_0 (1 - \exp(-\lambda \sigma)) . \tag{13}$$

Denoting $\Delta v_0 = \beta N_0$ we obtain the following formula

$$v = v_0 + \Delta v_0 (1 - \exp(-\lambda \sigma)) , \tag{14}$$

where v_0 is the velocity at which the elastic wave propagates in the stress-free rock and λ is a common parameter in the two models. Eq.(14) describes a theoretical connection between the propagation velocity and rock pressure (Dobróka and Somogyi Molnár 2012). Similarly to the quality factor, the velocity as a function of stress starts from v_0 and according to the function $1-\exp(-\lambda\sigma)$ increases up to the value $v_{max}=v_0+\Delta v_0$. Consequently, the value $\Delta v_0 = v_{max}-v_0$ is a velocity range in which the propagation velocity varies from stress-free state up to the state characterized by high rock pressure (v_{max}).

4.2.3. Experimental samples

The quality factor model was tested on measurement data published in literature. Data sets measured on Berea sandstone (Toksöz *et al.* 1979), Rotbach sandstone (Lucet and Zinszner 1992), coal samples (Yu *et al.* 1993) and Hebron gneiss (Meglis *et al.* 1996) were processed. The spectral ratio technique (Toksöz *et al.* 1979) was used to determine quality factor and measurements were carried out beside varying pressure.

The Berea medium-grained sandstone sample (Toksöz *et al.* 1979) was composed of angular grains which showed microcracks and the grain contacts were somewhat jagged and were weakly cemented. It had a porosity of 16 percent, permeability of 75 mD, and an average bulk density of 2.61 g/cm³. X-Ray scanner images for Rotbach sandstone showed that the rock density appeared rather uniform without major heterogeneities. The samples used by Yu *et al.* (1993) were Upper Permian black coal samples which were originated from the Bulli Seam near Wollongong and their physical appearance was dull, fairly homogeneous and microbanded in the central locality. The medium-grained quartz-plagioclase-biotite gneiss sample was originated from the Hebron formation. The sample had a subhorizontal metamorphic foliation which had influenced the orientation of microcracks.

Both quality factor and longitudinal velocity - as a function of pressure - were measured at adjoining pressures on Berea sandstone sample by Prasad and Manghnani (1997). Similarly the spectral ratio technique was used for quality factor measurements and the pulse transmission technique (Toksöz *et al.* 1979) was applied for velocity measurements. The analyzed Berea sandstone sample was composed of angular grains (150–200 μm) which showed microcracks. The grain contacts were somewhat jagged and were weakly cemented.

4.2.4. Estimation of model parameters appearing in the model

The petrophysical constants ($Q_0, \Delta Q_0, \lambda, v_0, \Delta v_0$) appearing in the model equations (Eq.(7) and Eq.(14)) can be determined by using inversion methods in processing the measurement data. In formulating the inverse problem, we introduce the column vector of model parameters as

$$\mathbf{m} = \{Q_0, \Delta Q_0, \lambda\}^T, \quad (15)$$

where T denotes the transpose. The parameters appearing in Eq. (7) gives the possibility to calculate the quality factor at the k -th pressure (σ_k). Measured quality factor data are also represented in a column vector

$$\mathbf{d}^{obs} = \{Q_l^{(obs)}, \dots, Q_{P_l}^{(obs)}\}^T, \quad (16)$$

where P_l is the number of the measured quality factor data. If the size of vector \mathbf{d} is larger than that of the vector \mathbf{m} , the inverse problem is overdetermined. Observations are connected to the model nonlinearly as

$$\mathbf{d}^{calc} = \mathbf{g}(\mathbf{m}), \quad (17)$$

where \mathbf{g} represents the model response function (given by Eq.(7)), which is used to calculate quality factor data at a pressure value and

$$\mathbf{d}^{calc} = \{Q_l^{(calc)}, \dots, Q_{P_l}^{(calc)}\}^T. \quad (18)$$

The function \mathbf{g} represents a nonlinear vector-vector function in the general case. If we approximate it with the first two members of its Taylor-series in any point not too far from the solution we can linearize the inverse problem. Then, the solution of the inverse problem can be found at the minimal distance between the measured and calculated data

$$\mathbf{E} = (\mathbf{e}, \mathbf{e}) = \min., \quad (19)$$

where

$$\mathbf{e} = \mathbf{d}^{obs} - \mathbf{d}^{calc}. \quad (20)$$

The Gaussian Least Squares method can be effectively used for solving overdetermined inverse problems (Menke 1984). In the inversion procedure the actual model is gradually refined until the best fitting between measured and calculated data is achieved

$$\mathbf{m} = \mathbf{m}_0 + \delta \mathbf{m}, \quad (21)$$

where \mathbf{m}_0 is the initial model and $\delta\mathbf{m}$ is the model correction vector. The vector of model corrections can be computed as

$$\delta\mathbf{m} = (\mathbf{G}^T \mathbf{G})^{-1} \mathbf{G}^T \delta\mathbf{d}, \quad (22)$$

where \mathbf{G} denotes the Jacobi's matrix, and $\delta\mathbf{d}$ is the difference between the measured and actually computed data vector. Solving the upper equation the new parameter vector can be given as

$$\mathbf{m}^{new} = \mathbf{m}^{old} + \delta\mathbf{m}. \quad (23)$$

The iterative procedure is repeated for 50 iteration step but from circa the 10th step the optimal parameters can be obtained for the actual inverse problem.

The described method was applied to process quality factor data sets. Eq.(7) was applied as a forward modelling formula and since the number of measured data is larger than that of parameters to be determined, the Least Squares method was used. The inversion procedure was numerically stable and could be handled properly by the above detailed linear inversion technique.

The velocity and quality factor data sets measured by Prasad and Manghnani (1997) was processed by using a joint inversion technique (Dobróka *et al.* 1991). In a joint inversion procedure we integrate all of the measurement data into one combined data vector and we give an estimate for the quality factor and velocity data in a single inversion algorithm, where λ is a common petrophysical parameter connecting the two data sets. Eq.(7) and Eq.(14) serve as forward modelling equations (model response functions) in handling the least squares-based joint inversion problem.

Results of the applied linearized inversion methods for each sample can be seen in Table 1. The estimation errors of the model parameters were calculated using the method given by Menke (1984). In the inverse problem let us assume that the linear connection of data (\mathbf{d}) and parameter space (\mathbf{m}) can be described by the equation

$$\mathbf{m} = \mathbf{A}\mathbf{d}, \quad (24)$$

where \mathbf{A} is the generalized inverse matrix of the current inversion method (in this case $(\mathbf{G}^T \mathbf{G})^{-1} \mathbf{G}^T$). Since \mathbf{A} does not depend on the measurement data, it can be deduced that

$$cov(\mathbf{m}) = \mathbf{A} cov(\mathbf{d}) \mathbf{A}^T, \quad (25)$$

which connects the covariance matrix of data space to that of the model space.

Table 1.: Model parameters with their estimation errors given by inversion procedure

Sample	Estimated petrophysical model parameters					D (%)
	Q ₀	ΔQ ₀	λ (1/MPa)	Δv ₀ (km/s)	v ₀ (km/s)	
Berea, dry (Toksöz <i>et al.</i> 1979)	21,22 (±0,91)	91,69 (±0,94)	0,0502 (±0,0022)	-	-	2,11
Rotbach (Lucet and Zinszner 1992)	10,24 (±1,49)	50,13 (±1,43)	0,0625 (±0,0097)	-	-	7,11
Coal No. 15 (Yu <i>et al.</i> 1993)	24,65 (±0,39)	35,59 (±0,40)	0,1122 (±0,0055)	-	-	1,84
Coal No. 17 (Yu <i>et al.</i> 1993)	6,67 (±0,51)	43,65 (±0,52)	0,0549 (±0,0027)	-	-	1,75
Hebron (Meglis <i>et al.</i> 1996)	7,21 (±0,55)	28,88 (±0,59)	0,0380 (±0,0030)	-	-	4,43
Berea, dry (Prasad and Manghnani 1997)	16,17 (±1,48)	55,66 (±1,84)	0,0911 (±0,0091)	0,89 (±0,05)	3,75 (±0,04)	5,59

For the covariance matrix in data space it is a general assumption that data are uncorrelated and the variance is the same for each data, thus

$$cov(\mathbf{d}) = \sigma_{(d)}^2 \mathbf{I}, \quad (26)$$

where \mathbf{I} is the identity matrix and $\sigma_{(d)}^2$ is the variance of the data. However, in case of different data sets (namely the quality factor and velocity data) it takes the form

$$cov(\mathbf{d}) = \begin{bmatrix} \sigma_1^2 & \dots & 0 & 0 & \dots & 0 \\ \vdots & \ddots & \vdots & \vdots & \ddots & \vdots \\ 0 & \dots & \sigma_1^2 & 0 & \dots & 0 \\ 0 & \dots & 0 & \sigma_2^2 & \dots & 0 \\ \vdots & \ddots & \vdots & \vdots & \ddots & \vdots \\ 0 & \dots & 0 & 0 & \dots & \sigma_2^2 \end{bmatrix} \quad (27)$$

where σ_1^2 denotes the variance of quality factor data and σ_2^2 means that of velocity data, respectively. At the end of the inversion procedure uncertainty for the estimates can be calculated from the deviations of measured and predicted data. Hence the elements of the main diagonal of covariance matrix in parameter space provides the variances of model parameters, that means

$$\sigma_{m_i} = \sqrt{\text{cov}(\mathbf{m})_{ii}} \quad (28)$$

gives the estimation error of the i-th model parameter (i=1,...,5 in the given problem). The estimation errors of the model parameters of each sample can be seen in parentheses in Table 1.

From the normalization of the elements of the covariance matrix one can derive the correlation matrix, which provides the strength of linear relationships between each pair of model parameters. The element of i-th row and j-th column of the correlation matrix is the correlation coefficient

$$\text{corr}(\mathbf{m})_{ij} = \frac{\text{cov}(\mathbf{m})_{ij}}{\sqrt{\text{cov}(\mathbf{m})_{ii} \text{cov}(\mathbf{m})_{jj}}}, \quad (29)$$

which characterizes the correlation of the related model parameters by a number in the interval [-1,1]. The correlation matrix can be characterized by a single scalar, which is the mean spread

$$S = \sqrt{\frac{1}{M(M-1)} \sum_{i=1}^M \sum_{j=1}^M (\text{corr}(\mathbf{m})_{ij} - \delta_{ij})^2}, \quad (30)$$

where δ is a Kronecker-delta symbol (which equals 1 if i=j, otherwise it is 0).

The correlation matrix in case of the joint inversion procedure (joint interpretation of quality factor and velocity data sets) can be seen in Table 2. For the identification of the parameter pairs see the order of elements of the combined model parameter vector ($\mathbf{m} = \{Q_0, \Delta Q_0, \lambda, v_0, \Delta v_0\}^T$). It can be seen that the values of the correlation coefficients are mostly under ~0,5 for each pairs of model parameters, which means that the estimated parameters are in connection i.e. are correlated moderately but the results are still reliable. The mean spread is obtained 0,3788, which also confirms the reliability of the inversion results. In order to prove the advantages of the joint inversion method we processed the measurement data of Berea sandstone (Prasad and Manghnani (1997)) by two single inversion procedures separately, of which results can be seen in Table 3. At the end of the inversion procedure the mean spreads are calculated. It is obtained 0,3793 for the velocity data set and 0,44 for the quality

factor data, respectively. It can be seen that as a result of applying a joint inversion method the inversion results can be improved, the mean spread can be reduced and the reliability of the inversion result can be increased.

Table 2.: Values of the calculated measure of fitting in data space

Correlation matrix of model parameters estimated by the joint inversion method					
$corr(\mathbf{m}) =$	$\begin{bmatrix} 1.0000 & -0.1720 & 0.0540 & -0.7753 & 0.0880 \\ -0.1720 & 1.0000 & -0.3138 & -0.3002 & -0.5120 \\ 0.0540 & -0.3138 & 1.0000 & 0.0942 & -0.5571 \\ -0.7753 & -0.3002 & 0.0942 & 1.0000 & 0.1537 \\ 0.0880 & -0.5120 & -0.5571 & 0.1537 & 1.0000 \end{bmatrix}$				

4.2.5. Inversion results

By means of (joint) inversion-based processing introduced in the previous section the model parameters were determined from measurement data. The inverse problem was significantly overdetermined; hence the inversion procedure was numerically stable and could be handled by a linear inversion technique. With the estimated parameters the quality factors and acoustic velocities can be determined at any pressure by means of the developed model equations. Figs. 1-5 represent the results – in case of quality factor data – and Fig. 6 shows the joint inversion results. For making a comparison, Fig. 7 represents the results of the single inversion procedures of the Berea sample. In the figures solid lines show the calculated function, while asterisks represent the measured data. Figs. 1-7 show that the calculated curves are in good accordance with the measured data, which proves that the suggested petrophysical models for the explanation of the exponential relationship between the seismic Q/velocity and rock pressure apply well in practice.

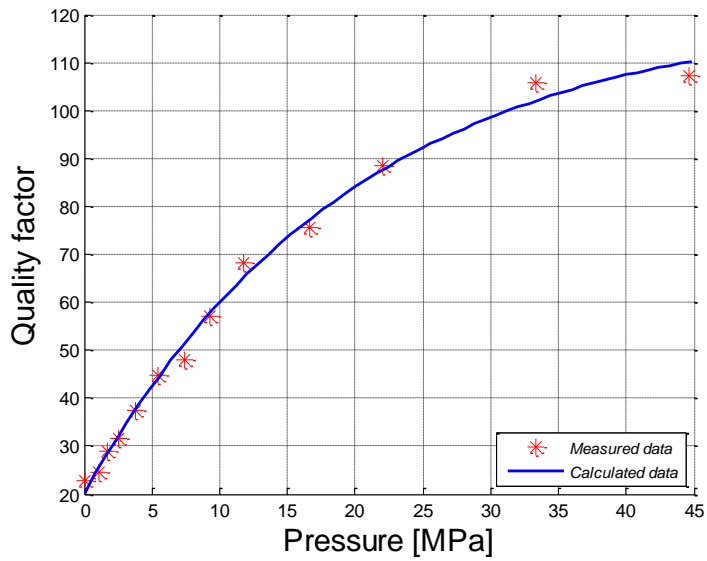


Figure 1.: Pressure dependence of compressional wave quality factor in Berea sandstone sample. Data obtained from Toksöz et al. (1979). Solid line represents the calculated data: results of inversion processing using the quality factor model; asterisks show the measured data.

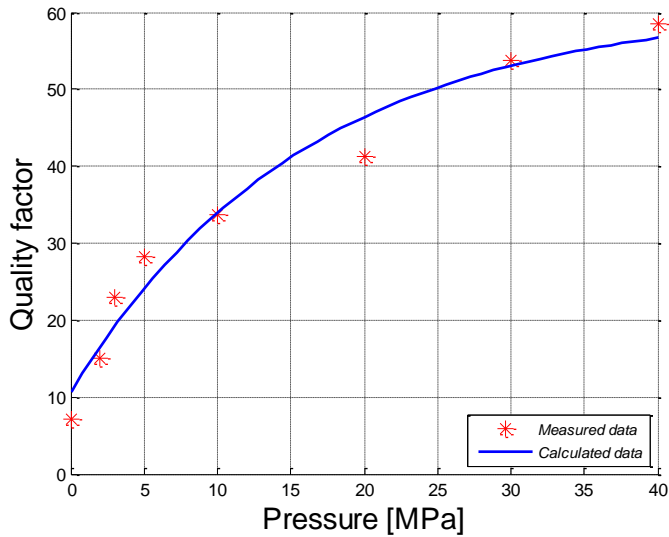


Figure 2.: Pressure dependence of compressional wave quality factor in Rotbach sandstone sample. Data obtained from Lucet and Zinszner (1992). Solid line represents the calculated data: results of inversion processing using the quality factor model; asterisks show the measured data.

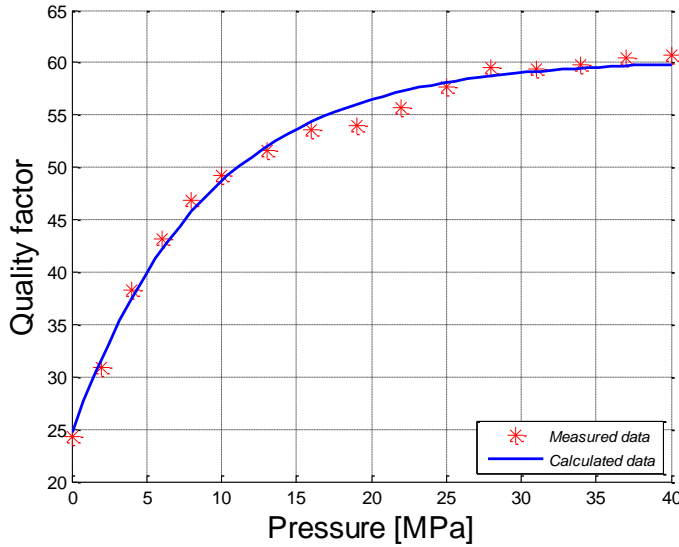


Figure 3.: Pressure dependence of compressional wave quality factor in Coal No. 15 sample. Data obtained from Yu et al. (1993). Solid line represents the calculated data: results of inversion processing using the quality factor model; asterisks show the measured data.

It can be seen also in the figures that in the lower pressure regime – which is the most important range in near-surface problems such as mining, geotechnics, oil exploration, etc. -, the increase in quality factor and longitudinal velocity with increasing pressure is very steep and nonlinear; this is due to the closure of microcracks. In the higher pressure regime, the increase in quality factor and velocity (with increasing pressure) is moderate as fewer numbers of cracks are available for closing.

For the characterization of the accuracy of estimations, the measure of fitting in data space was calculated according to the data misfit formula (Dobróka *et al.* 1991)

$$D = \sqrt{\frac{1}{N} \sum_{k=1}^N \left(\frac{d_k^{(m)} - d_k^{(c)}}{d_k^{(c)}} \right)^2} \cdot 100 [\%], \quad (31)$$

where $d_k^{(m)}$ is the measured quality factor and seismic velocity at the k-th pressure value and $d_k^{(c)}$ is the k-th calculated quality factor and seismic velocity data, which can be computed according to Eq.(7) or rather Eq.(14). Tables 2-3. contain the obtained percentages.

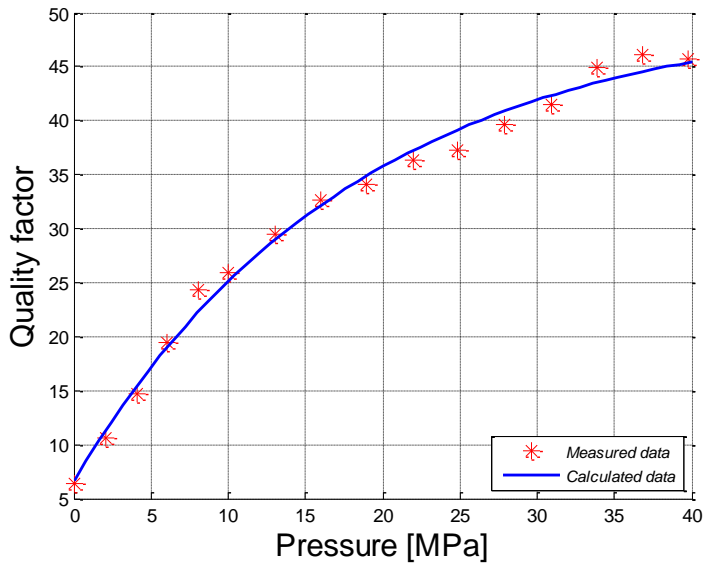


Figure 4.: Pressure dependence of compressional wave quality factor in Coal No. 17 sample. Data obtained from Yu et al. (1993). Solid line represents the calculated data: results of inversion processing using the quality factor model; asterisks show the measured data.

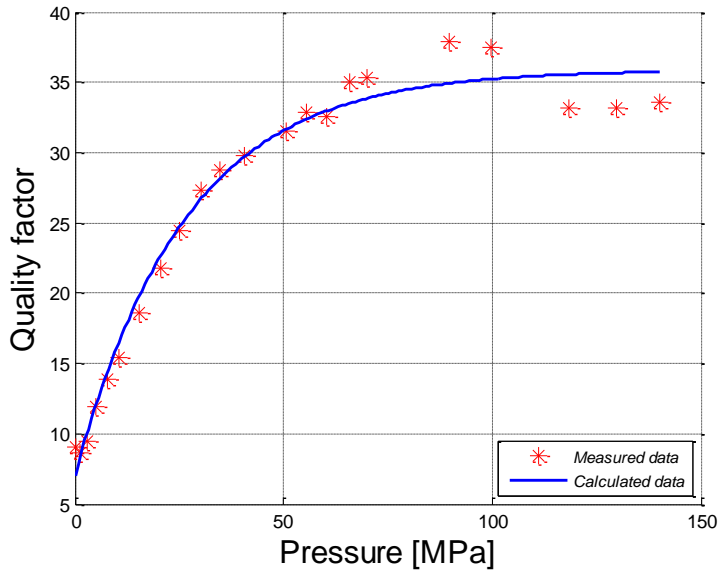


Figure 5.: Pressure dependence of compressional wave quality factor in Hebron gneiss sample. Data obtained from Meglis et al. (1996). Solid line represents the calculated data: results of inversion processing using the quality factor model; asterisks show the measured data.

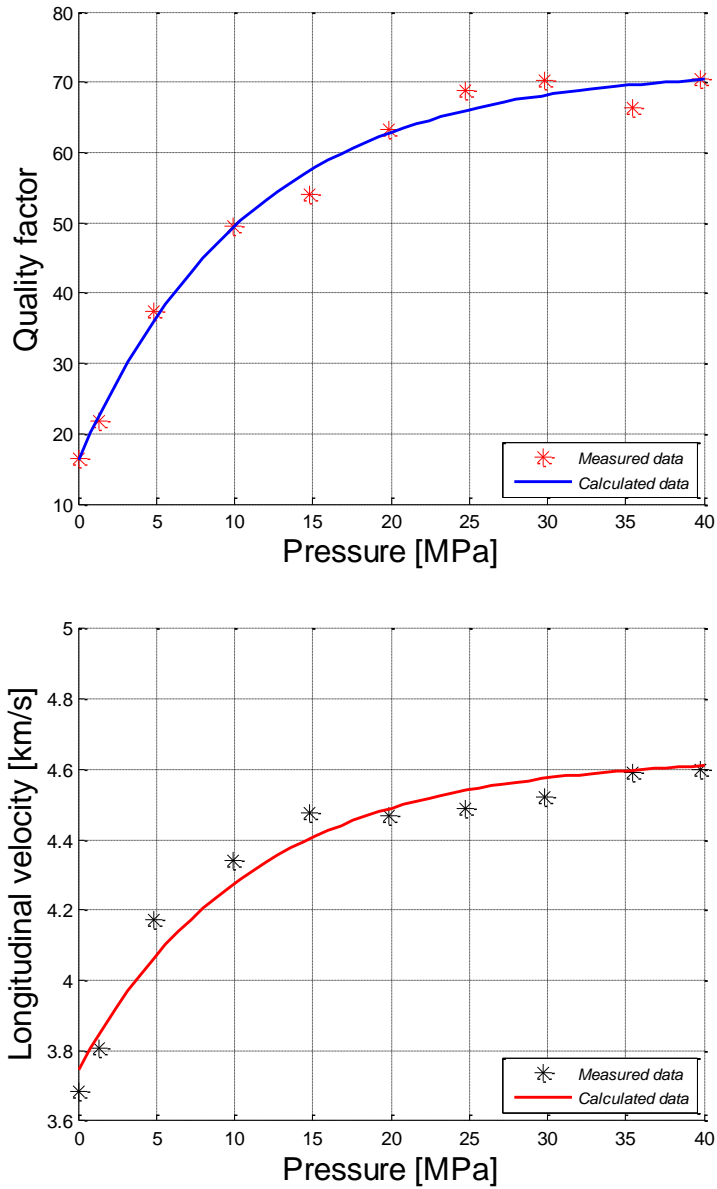


Figure 6.: Pressure dependence of quality factor and seismic velocity of compressional wave in Berea sandstone sample. Data adopted from Prasad and Manghnani (1997). Solid line represents the calculated data: results of inversion processing using the quality factor model; asterisks show the measured data.

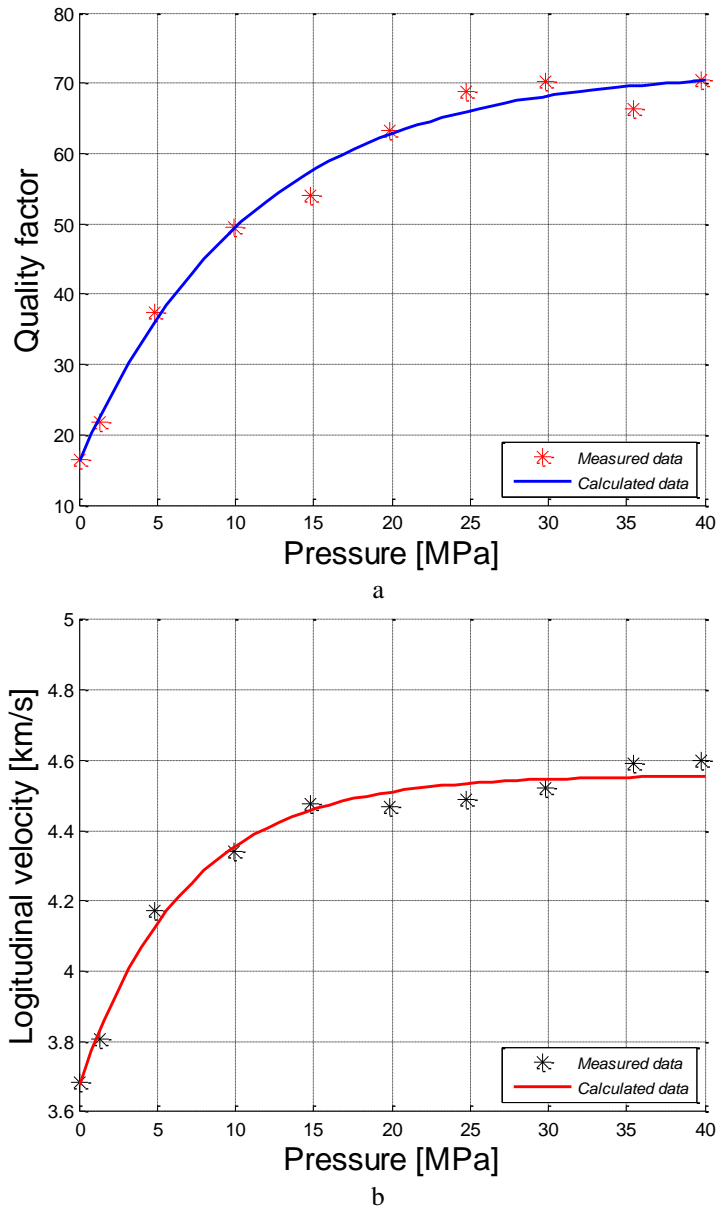


Figure 7.: Pressure dependence of quality factor (a) and seismic velocity (b) of compressional wave in Berea sandstone sample. Data taken over from Prasad and Manghnani (1997). Solid line represents the calculated data: results of inversion processing using the quality factor model; asterisks show the measured data.

Table 3.: Model parameters with their estimation errors calculated by two single inversion procedures using Berea sandstone

Sample	Estimated petrophysical model parameters					D (%)
	Q ₀	ΔQ ₀	λ (1/MPa)	Δv ₀ (km/s)	v ₀ (km/s)	
Berea, dry (Prasad and Manghnani 1997)	16,14 (±0,86)	54,81 (±1,15)	0,0907 (±0,0031)	-	-	2,51
Berea, dry (Prasad and Manghnani 1997)	-	-	0,1477 (±0,0115)	0,88 (±0,01)	3,67 (±0,01)	2,34

The fitting in case of processed quality factor data sets was under 4.5% except for the Rotbach sample. The inversion would have been more accurate – and resulted in smaller value - at that sample, if quality factor had been measured beside more pressure values. By the joint inversion method the fitting between measured and calculated data was 5.59%. However, by using a joint inversion method the mean spread can be reduced, on the other hand the fitting can be improved. Based on Figs. 6-7 one can see that the reason of the latter is originated from the velocity data set. Even so the noise in data space is small-scale, which confirms the accuracy of the inversion result and the feasibility of the developed petrophysical models.

References

- Bastiaens W. 2005. EDZ around an industrial excavation in Boom Clay. In: Davies C. and Bernier F. (eds): EDZ around an industrial excavation in Boom Clay, Luxembourg, 305-309.
- Best A.I. 1997. The effect of pressure on ultrasonic velocity and attenuation in near-surface sedimentary rocks. *Geophysical Prospecting* 45, 345-364. doi:10.1046/j.1365-2478.1997.00344
- Biot M.A. 1956a. Theory of propagation of elastic waves in a fluid-saturated porous solids, I: Low frequency range. *Journal of the Acoustical Society of America* 28, 168-178. doi:10.1121/1.1908239

- Biot M.A. 1956b. Theory of propagation of elastic waves in a fluid-saturated porous solids, II: High frequency range. *Journal of the Acoustical Society of America* 28, 179-191. doi:10.1121/1.1908241
- Birch F. 1960. The velocity of compression waves in rocks to 10 kilobars, Part 1. *Journal of Geophysics Research* 65, 1083-1102. doi:10.1029/JZ065i004p01083
- Bland D.R. 1960. *The theory of linear viscoelasticity*, Pergamon Press, Oxford.
- Bourbié C.T., Coussy O. and Zinszner B. 1987. *Acoustics of porous media*, Gulf Publ. Co., Paris.
- Brace W.F. and Walsh J.B. 1964. A fracture criterion for brittle anisotropic rock. *Journal of Geophysics Research* 69, 3449-3456. doi:10.1029/JZ069i016p03449
- Dobróka M., Gyulai Á., Ormos T., Csókás J. and Dresen L. 1991. Joint inversion of seismic and geoelectric data recorded in an underground coal-mine. *Geophysical Prospecting* 39, 643-665. doi:10.1111/j.1365-2478.1991.tb00334
- Dobróka M. and Somogyi Molnár J. 2012. New petrophysical model describing the pressure dependence of seismic velocity. *Acta Geophysica* 60(2), 371-383. doi: 10.2478/s11600-011-0079-0
- Dunn K.J. 1987. Sample boundary effect in acoustic attenuation of fluid-saturated porous cylinders. *Journal of the Acoustical Society of America* 81, 1259- 1266.
- Gordon R. B. and Davis L. A. 1968. Velocity and attenuation of seismic waves in imperfectly elastic rock. *Journal of Geophysical Research* 73, 3917-3935. doi: 10.1029/JB073i012p03917
- Gyulai Á. 1989. Parameter sensitivity of underground DC measurements. *Geophysical Transactions* 35(3), 209-225.
- Hamilton E.L. 1976. Sound attenuation as a function of depth in the sea floor. *Journal of the Acoustical Society of America* 59(3), 528-535.
- Han T., Best A.I., Sothcott J. and MacGregor L.M. 2011. Pressure effects on joint elastic-electrical properties of reservoir sandstones. *Geophysical Prospecting* 59, 506-517. doi:10.1111/j.1365-2478.2010.00939.x
- Hunter A. N., Legge R. and Matsukawa E. 1961. Measurements of acoustic attenuation and velocity in sand. *Acoustica* 11(1), 26-31.
- Ji S., Wang Q. Marcotte D., Salisbury M.H. and Xu Z. 2007. P wave velocities, anisotropy and hysteresis in ultrahigh-pressure metamorphic rocks as a function of confining pressure. *Journal of Geophysical Research* 112, B09204, doi: 10.1029/2006JB004867.

- Johnston D.H., Toksöz M.N. and Timur A. 1979. Attenuation of seismic waves in dry and saturated rocks, II. Mechanism. *Geophysics* 44(4), 691-711. doi:10.1190/1.1440970
- Klíma K., Vanek I. and Pros Z. 1964. The attenuation of longitudinal waves in diabase and greywacke under pressures up to 4 kilobars. *Studia Geophysica et Geodetica* 8, 247–254. doi: 10.1007/BF02607174
- Khazanehdari J. and McCann C. 2005. Acoustic and petrophysical relationships in low-shale sandstone reservoir rocks. *Geophysical Prospecting* 53, 447–461. doi: 10.1111/j.1365-2478.2005.00460.x
- Knopoff L. 1965. Attenuation of elastic waves in the earth. In: Mason W. S. (ed): *Physical acoustics*, Academic Press, New York. IIIB, 287–324.
- Kuster G. and Toksöz M. N. 1974. Velocity and attenuation of seismic waves in two-phase media, part I: Theoretical formulations. *Geophysics* 39, 587–606.
- Lucet N., Rasolofosaon N.J.P. and Zinszner B. 1991. Sonic properties of rocks under confining pressure using the resonant bar technique. *Journal of the Acoustical Society of America* 89, 980-990.
- Lucet N. and Zinszner B. 1992. Effects of heterogeneities and anisotropy on sonic and ultrasonic attenuation in rocks. *Geophysics* 57(8), 1018-1026. doi:10.1190/1.1443313
- Mavko G.M., Kjartansson E. and Winkler K. 1979. Seismic wave attenuation in rocks. *Reviews of Geophysics and Space Physics* 17, 1155-1164.
- Meglis I.L., Greenfield R.J., Engelder T. and Graham E.K. 1996. Pressure dependence of velocity and attenuation and its relationship to crack closure in crystalline rocks. *Journal of Geophysical Research* 101(B8), 17523-17533. doi:10.1029/96JB00107
- Menke W. 1984. *Geophysical data analysis – Discrete inverse theory*, Academic Press, London.
- Murphy W.F. 1982. Effects of partial water saturation on attenuation in Massillon sandstone and Vycor porous glass. *Journal of the Acoustical Society of America* 71, 1458-1468.
- O'Doherty R. F. and Anstey N. A. 1971. Reflections on amplitudes. *Geophysical Prospecting* 19, 430–458. doi:10.1111/j.1365-2478.1971.tb00610.x
- Paffenholz J. and Burkhardt H. 1989. Absorption and modulus measurements in the seismic frequency and strain range on partially saturated sedimentary rocks. *Journal of Geophysical Research* 94, 9493-9507. doi:10.1029/JB094iB07p09493
- Prasad M. and Manghnani M.H. 1997. Effects of pore and differential pressure on compressional wave velocity and quality factor in Berea and Michigan sandstones. *Geophysics* 62(4), 1163-1176. doi:10.1190/1.1444217

- Prasad M. and Meissner R. 1992. Attenuation mechanisms in sands: Laboratory versus theoretical (Biot) data. *Geophysics* 57(5), 710–719. doi: 10.1190/1.1443284
- Schön J.H. 1996. Physical properties of rocks: fundamentals and principles of petrophysics. In: Helbig K. and Treitel S.(eds): *Handbook of Geophysical Exploration. Seismic exploration*, Pergamon Press, Trowbridge, Volume 18.
- Singh R., Rai C. and Sondergeld C. 2006. Pressure dependence of elastic wave velocities in sandstones. 76th International Exposition and Annual Meeting, SEG, Expanded Abstract, 1883-1887.
- Spencer J.W. 1981. Stress relaxations at low frequencies in fluid saturated rocks: attenuation and modulus dispersion. *Journal of Geophysical Research* 86, 1803-1812. doi:10.1051/jphyscol:19815182
- Toksöz M.N., Johnston D.H. and Timur A. 1979. Attenuation of seismic waves in dry and saturated rocks: I. Laboratory measurements. *Geophysics* 44(4), 681-690. doi:10.1190/1.1440969
- Toksöz M. N. and Johnston D.H. 1981. Preface. In: SEG Geophysics reprint series No. 2 *Seismic Wave Attenuation*, pp. 1–5. SEG Tulsa/Oklahoma
- Walsh J. B. 1966. Seismic wave attenuation in rock due to friction. *Journal of Geophysical Research* 71, 2591–2599. doi:10.1029/JZ071i010p02591
- Wang H., Todd T., Weidner D. and Simmons G. 1971. Elastic properties of Apollo 12 rocks. In: *Proc. 2-nd Lunar Science Conference*, vol. 3, Mass. Inst. Technol. Press, 2327–2336.
- Wang Q., Ji S.C., Salisbury M.H., Xia M.B., Pan B. and Xu Z.Q. 2005. Shear wave properties and Poisson's ratios of ultrahigh-pressure metamorphic rocks from the Dabie-Sulu orogenic belt: Implications for the crustal composition. *Journal of Geophysical Research* 110, B08208. doi:10.1029/2004JB003435
- Wepfer W.W. and Christensen N.I. 1991. A seismic velocity-confining pressure relation, with applications. *International Journal of Rock Mechanics and Mining Science* 28, 451–456.
- White J. E. 1966. Static friction as a source of seismic attenuation. *Geophysics* 31(2), 333–339. doi: 10.1190/1.1439773
- Winkler K. 1985. Dispersion analysis of velocity and attenuation in Berea sandstone. *Journal of Geophysical Research* 90, 6783-6800.
- Yu G., Vozoff K. and Durney D.W. 1993. The influence of confining pressure and water saturation on dynamic elastic properties of some Permian coals. *Geophysics* 58(1), 30-38. doi:10.1190/1.1443349